A natural genetic variation screen identifies insulin signaling, neuronal communication, and innate immunity as modifiers of hyperglycemia in the absence of *Sirt1*

Rebecca A.S. Palu

Biology Department, Purdue University-Fort Wayne, Fort Wayne, IN 46818

Running title: Natural modifiers of hyperglycemia

Key words: hyperglycemia, *Drosophila*, genetic variation, modifier genes

Corresponding author:

Rebecca A.S. Palu

Biology Department

Science Building SB330

2101 E. Coliseum Blvd

Fort Wayne IN, 46805

260-481-5704

palur@pfw.edu

ABSTRACT

Variation in the onset, progression, and severity of symptoms associated with metabolic disorders such as diabetes impairs the diagnosis and treatment of at-risk patients. Diabetes symptoms, and patient variation in these symptoms, is attributed to a combination of genetic and environmental factors, but identifying the genes and pathways that modify diabetes in humans has proven difficult. A greater understanding of genetic modifiers and the ways in which they interact with metabolic pathways could improve the ability to predict a patient's risk for severe symptoms, as well as enhance the development of individualized therapeutic approaches. In this study we use the *Drosophila* Genetic Reference Panel (DGRP) to identify genetic variation influencing hyperglycemia associated with loss of *Sirt1* function. Through analysis of individual candidate functions, physical interaction networks, and Gene Set Enrichment Analysis (GSEA) we identify not only modifiers involved in canonical glucose metabolism and insulin signaling, but also genes important for neuronal signaling and the innate immune response. Furthermore, reducing the expression of several of these candidates suppressed hyperglycemia, making them ideal candidate therapeutic targets. These analyses showcase the diverse processes contributing to glucose homeostasis and open up several avenues of future investigation.

INTRODUCTION

Metabolic diseases, and in particular diabetes, are one of the most pressing health crises in the developed world, with incidences continuing to rise in the last 20 years (CDC 2020). 37.7% of adults in the US are diagnosed as obese and 10.5% as having some form of diabetes, and it is estimated that millions more go undiagnosed (Flegal *et al.* 2016; CDC 2020). What is more, the monetary cost of these disorders to the public has grown to astronomical levels. It is estimated that $237 billion in direct costs and at least $90 billion in indirect costs were spent on healthcare related to diabetes and its various complications in 2017 alone, up ~25% from 2012 (Flegal *et*

53 *al.* 2016). A focused effort has been made to understand both the genetic and environmental
54 contributors to metabolic homeostasis, as well as to the disruption of that homeostasis that
55 leads to disease (Barroso and McCarthy 2019).
56
57 Unfortunately, even identifying these contributors has proven difficult. Metabolic diseases are
58 complex, and the onset, progression, and ultimately the severity of any individual case is
59 dependent upon a myriad of genetic and environmental variables and the ways in which they
60 interact with one another (Queitsch *et al.* 2012; Barroso and McCarthy 2019). Even when there
61 is a strong familial link, phenotypic heterogeneity in disease phenotypes can make it difficult to
62 identify at-risk patients or make accurate prognostic predictions (Udler *et al.* 2019). This is
63 particularly true when it comes to predicting complications of diabetes such as neuropathy,
64 retinopathy, or kidney disease (Barroso and McCarthy 2019; Cabrera *et al.* 2020). Much of this
65 variation is due to inter-individual differences in genetic background, including silent cryptic
66 genetic variation that is revealed upon disease or stress (Queitsch *et al.* 2012; Chow 2016;
67 Barroso and McCarthy 2019).
68
69 One example of this kind of symptom heterogeneity can be observed in disease associated with
70 the deacetylase *SIRT1*. This highly conserved gene was originally identified as a histone
71 deacetylase important in heterochromatin formation in yeast (Shore *et al.* 1984; Ivy *et al.* 1986;
72 Rine and Herskowitz 1987). Since then, SIRT1 and its paralogs (the sirtuins) have been found
73 to have a number of additional targets, many of which are transcription factors and enzymes
74 with key roles in metabolic homeostasis (Brunet *et al.* 2004; Picard *et al.* 2004; Rodgers and
75 Puigserver 2007; Li *et al.* 2007; Yang *et al.* 2009; Palu and Thummel 2016). Importantly, as part
76 of their enzymatic reaction, sirtuins consume the cofactor NAD, which also serves as an
77 electron carrier in central metabolic pathways such as glycolysis and the TCA cycle. Sirtuin
78 enzymatic activity, therefore, is directly linked to the availability of this cofactor and thus is

responsive to the energetic state of the cell. This information is then conveyed to the targets, whose acetylation state alters their activity and stability in the cell (Nogueiras *et al.* 2012). With this centralized role in regulating the response of metabolic factors to cellular energy availability, it is unsurprising that variation in *SIRT1* has been linked to, among other things, the development of diabetes (Zillikens *et al.* 2009; Botden *et al.* 2012; Biason-Lauber *et al.* 2013; Zhao *et al.* 2017).

Elucidating the mechanism behind this link, however, has proven difficult. Loss-of-function and gain-of-function studies in model systems have demonstrated a clear role for SIRT1 in metabolic homeostasis, but the actual impacts on the animals in question have frequently been contradictory (Boutant and Cantó 2014). It is likely that at least some of these contradictory results stem from differences in genetic background between the animals used in the various studies. Understanding the role of this variation and the genes or pathways which modify metabolic disease will enable the development of improved diagnosis, prediction of prognosis, and personalized treatment strategies for patients.

Model organism tools, such as the *Drosophila* Genetic Reference Panel (DGRP), provide a way to study of the impact of natural genetic variation on diseases such as diabetes (Mackay *et al.* 2012; He *et al.* 2014; Ivanov *et al.* 2015; Nelson *et al.* 2016; Jehrke *et al.* 2018; Everman *et al.* 2019). The DGRP is a collection of ~200 isogenic strains derived from a wild population, such that each strain represents one wild-derived genome (Mackay *et al.* 2012). The variation in the DGRP is well tolerated under healthy, non-disease conditions and allows for the identification of genetic polymorphisms that are associated with phenotypic variation in models of human disease (Chow and Reiter 2017). Importantly, the availability of full-genome sequence for these strains allows for genome-wide association analyses that link quantitative phenotypes with genetic variation and modifier genes.

105

106 The utility of the DGRP in identifying candidate modifiers of metabolic disease has already been
107 demonstrated numerous times, with screens associated with misfolded insulin, high sugar and
108 high fat feeding, and starvation resistance already documented (Mackay *et al.* 2012; He *et al.*
109 2014; Ivanov *et al.* 2015; Nelson *et al.* 2016; Jehrke *et al.* 2018; Everman *et al.* 2019). While
110 some of these used biochemical assays to precisely measure metabolite levels in flies as a
111 quantitative phenotype for the screen (Nelson *et al.* 2016; Jehrke *et al.* 2018; Everman *et al.*
112 2019), several used more general physiological measurements such as starvation resistance
113 and lifespan (Mackay *et al.* 2012; Ivanov *et al.* 2015). Although effective, the use of this kind of
114 general readout reduces the specificity of the modifiers identified. Many genetic factors impact
115 survival and could lead to a high background signal. The same could be true for otherwise wild-
116 type flies subjected to different environmental conditions, even when more precise assays are
117 used as a quantitative phenotype (Nelson *et al.* 2016). A multitude of pathways and processes
118 impact the response to dietary changes through feeding rate, hormone secretion, anabolism
119 and catabolism rates, and nutrient absorption. Using a specific genetic model of disease and
120 then focusing on a specific phenotype, such as hyperglycemia, may reduce some of the noise
121 and increase specificity of the modifiers identified.
122

123 Furthermore, recent studies using the DGRP have demonstrated that the top candidate modifier
124 genes and pathways differ when different but related models of genetic disease are screened
125 (Chow *et al.* 2016; Palu *et al.* 2019). These results reinforce the idea that different causative
126 genes and mutations will interact with different pathways over the course of disease. It also
127 highlights the importance of exploring multiple disease models in something so diverse as
128 diabetes, and the utility of the DGRP in precisely distinguishing modifiers of a particular
129 genotype-phenotype combination.
130

131 In this study, we report the results of a natural variation screen in a model of *Sirt1* loss-of-
132 function. Loss of this gene in *Drosophila* has been shown to lead to progressive metabolic
133 dysfunction including obesity, hyperglycemia, and ultimately insulin resistance (Palu and
134 Thummel 2016). Our study design is specifically focused on the phenotype of hyperglycemia
135 when *Sirt1* expression is disrupted using RNAi in the adipose and liver-like fat body organ. We
136 observed substantial phenotypic variation across the DGRP for hyperglycemia associated with
137 loss of *Sirt1*. Using genome-wide association analysis, pathway enrichment, and the generation
138 of a physical interaction network, we identified a number of modifying pathways and processes,
139 several of which have known roles in central carbon metabolism, the immune response, and the
140 kind of neuronal signaling and communication expected to influence the neuroendocrine cells
141 responsible for insulin secretion in *Drosophila*. Finally, we confirmed that loss of several of the
142 top candidate modifier genes significantly alters glucose levels in the *Sirt1* RNAi model. Our
143 findings highlight exciting new areas of study for modifiers of *Sirt1* function, glucose
144 homeostasis, and insulin sensitivity.
145

146 **METHODS**

147 *Fly stocks and maintenance*

148 Flies were raised at room temperature on a diet based on the Bloomington Stock Center
149 standard medium with malt. Experimental crosses were maintained on a media containing 6%
150 yeast, 6% dextrose, 3% sucrose, and 1% agar, with 0.6% propionic acid and 0.1% p-Hydroxy-
151 benzoic acid methyl ester in 95% ethanol included as antifungal agents. Flies subjected to an
152 overnight fast were transferred to media containing only 1% agar in water. The *R4>Sirt1i* strain,
153 which serves as the model of hyperglycemia in this study, is derived from an *R4-GAL4* strain
154 (BDSC 33832) outcrossed to w^{1118} (Palu and Thummel 2016) and a *Sirt1* RNAi strain from the
155 Bloomington Stock Center (32481). 185 strains from the DGRP were used for the modifier
156 screen (Tables S1-S3), wherein virgin females carrying the *R4>Sirt1i* model were crossed to

157 males of the DGRP strains. Male F1 progeny carrying *R4>Sirt1i* were separated and aged for
158 one to two weeks. These flies were then either collected under ad libitum fed conditions or
159 fasted overnight and then collected. The following RNAi and control strains are from the
160 Bloomington Stock Center: *CG4168* RNAi (28636), *CG5888* RNAi (62175), *uif* RNAi (38354),
161 *CTPSyn* RNAi (31924), *smt3* RNAi (36125), *ilp5* RNAi (33683), *Vha55* RNAi (40884), *snRNP-*
162 *U1-70k* RNAi (33396), *CG10265* RNAi (43294), *CG15803* RNAi (51449), *Roe* RNAi (57836),
163 *CG34353* RNAi (58291), *CadN2* RNAi (27508), *Ace* RNAi (25958), *CG43897* (31560), *dsxc73A*
164 RNAi (56987), *bgm* RNAi (56979), *CG3407* RNAi (57762), control *attP40* (36304), and control
165 *attP2* (36303).
166
167 *Glucose Assay*
168 Samples of five flies each were collected at one or two weeks of age and washed in 1XPBS.
169 Samples were then either frozen in liquid nitrogen and stored long-term at -80C or immediately
170 homogenized in 100 uL 1X PBS. Frozen samples were kept frozen until immediately upon
171 addition of PBS and homogenization. After homogenization samples were subjected to heat
172 inactivation of enzymes at 70C for approximately 10 minutes. Glucose was measured undiluted
173 from the lysate using the Sigma HK Glucose Assay kit as described (Tennessen *et al.* 2014).
174
175 *Protein Assay*
176 Prior to heat inactivation, 10 uL of the fly lysate isolated for glucose measurement was saved
177 and kept on ice. Protein samples could then be stored long term at -80ºC. Samples were
178 centrifuged for up to 5 minutes at room temperature and protein measured from the supernatant
179 after a 1:10 dilution using the Sigma Protein Assay Reagent as described (Tennessen *et al.*
180 2014).
181
182 *Phenotypic analysis and genome-wide association*

For each DGRP line, glucose was measured from 3 samples of 5 flies each. The P-values for association of genetic background and glucose concentration were calculated using one-way ANOVA on R software taking into account all collected data points for each experiment. Average glucose concentration was used for the genome-wide association (GWA). GWA was performed as previously described (Chow *et al.* 2016; Palu *et al.* 2019). DGRP genotypes were downloaded from the website, http://dgrp.gnets.ncsu.edu/. Non-biallelic sites were removed. A total of 3,636,891 variants were included in the analysis. Mean eye glucose concentration for 555 samples representing 2775 DGRP/R4>Sirt1i F1 progeny were regressed on each SNP. To account for cryptic relatedness (He *et al.* 2014; Huang *et al.* 2014), GEMMA (v. 0.94) (Zhou and Stephens 2012) was used to both estimate a centered genetic relatedness matrix and perform association tests using the following linear mixed model (LMM):

$$y=\alpha+x\beta+u+\epsilon$$

$$u \sim MVN_n (0,\lambda\tau^{-1} K)$$

$$\epsilon \sim MVN_n (0,\tau^{-1} I_n)$$

where, as described and adapted from Zhou and Stephens 2012, y is the n-vector of average glucose concentration for the n lines, α is the intercept, x is the n-vector of marker genotypes, β is the effect size of the marker. u is a n x n matrix of random effects with a multivariate normal distribution (MVN_n) that depends on λ, the ratio between the two variance components, τ^{-1}, the variance of residuals errors, and where the covariance matrix is informed by K, the calculated n x n marker-based relatedness matrix. K accounts for all pairwise non-random sharing of genetic material among lines. ϵ, is a n-vector of residual errors, with a multivariate normal distribution that depends on τ^{-1} and I_n, the identity matrix. Quantile-quantile (qq) plots demonstrate an appropriate fit to the LMM at the positive end of the plot, but a greater number of points than expected by chance with an insignificant p-value (Figure S1). Genes were identified from SNP coordinates using the BDGP R54/dm3 genome build. A SNP was assigned to a gene if it was +/- 1 kb from a gene body.

209

210 *RNAi Validation*

211 Virgin females from the *R4>Sirt1i* model were crossed to males carrying RNAi constructs
212 targeting candidate modifiers of those models, and the glucose levels of F1 male progeny
213 expressing both *Sirt1i* and the modifier RNAi construct specifically in the fat body were
214 measured as described above on 4-5 samples of 5 male flies each. Glucose concentrations
215 from RNAi-carrying strains are compared directly to genetically matched *attP40* or *attP2*
216 controls using a Dunnett's multiple comparisons test. Glucose measurements are normalized to
217 the appropriate genetically matched controls. Normalized controls from individual experiments
218 are compared in Figure S2. Standard deviation did not significantly vary between controls for
219 individual experiments.

220

221 *Bioinformatics Analysis*

222 Genetic polymorphisms were associated with candidate genes within 1 kb of the polymorphism.
223 Information about candidate genes and their human orthologues was gathered from a number
224 of databases including Flymine, Flybase, OMIM, and NCBI. Physical interaction maps were
225 generated using the GeneMANIA plugin on Cytoscape (version 3.8.2) (Shannon *et al.* 2003;
226 Montojo *et al.* 2010). GSEA was run to generate a rank-list of genes based on their enrichment
227 for significantly associated polymorphisms. For GSEA analysis, polymorphisms within 1kb of
228 more than 1 gene were assigned to one gene based on a priority list of exon, UTR, intron, and
229 upstream or downstream. Genes were assigned to GO categories, and calculation of
230 enrichment score was performed as described (Subramanian *et al.* 2005). Categories with ES
231 scores > 0 (enriched for associated genes with low p-values), gene number > 3, and p-values
232 <0.05 were included in the final output.

233

234 **RESULTS**

235 *Glucose levels in R4>Sirt1i flies vary with genetic background in a consistent pattern across*
236 *multiple conditions*
237 Loss of *Sirt1* expression leads to progressive hyperglycemia, obesity, and insulin resistance. To
238 model the hyperglycemia that is commonly associated with diabetes, we reduced the
239 expression of the deacetylase *Sirt1* specifically in the fat body of *Drosophila melanogaster*.
240 RNAi targeting *Sirt1* specifically in the fat body reproduces the hyperglycemia phenotype, with
241 an approximately 50-60% increase in whole fly glucose levels (P = 0.02, Figure S3) (Palu and
242 Thummel 2016). The fat body in *Drosophila* performs functions normally undertaken by the
243 adipose and liver tissues in humans (Géminard *et al.* 2009; DiAngelo and Birnbaum 2009;
244 Arrese and Soulages 2010). While there are likely roles for *Sirt1* in other metabolic tissues, its
245 function in the fat body clearly contributes to the maintenance of glucose homeostasis and
246 insulin sensitivity over time (Palu and Thummel 2016). Modifiers of insulin signaling or glucose
247 metabolism could alter the degree of hyperglycemia in this model.
248
249 The degree of hyperglycemia is determined by a biochemical assay that measures the
250 concentration of glucose in a whole-fly lysate (Tennessen *et al.* 2014). This is a quantitative
251 assay where higher concentrations of glucose correlate with more severe hyperglycemia, and
252 lower concentrations of glucose correlate with milder disease, or potentially hypoglycemia.
253 Glucose was measured specifically in males, as adult female *Drosophila* devote much of their
254 physiological output to egg production (Millington and Rideout 2018). Previous studies have
255 demonstrated that adult males provide a consistent model for metabolic homeostasis in the fly
256 (Sieber and Thummel 2009; Tennessen *et al.* 2014; Palu and Thummel 2016; Barry and
257 Thummel 2016; Beebe *et al.* 2020).
258
259 Loss of *Sirt1* is induced using the *GAL4/UAS* system, where *R4-GAL4* drives expression of
260 *UAS-Sirt1* RNAi (Figure S4A). *R4-GAL4* is strongly expressed primarily in the fat body of fly,

261 starting in early development and continuing through adulthood (Lee and Park 2004). The line
262 containing this model (*R4>Sirt1i*) serves as the donor strain that was crossed to each DGRP
263 strain. Females from the donor strain were crossed with males of each of 185 DGRP strains to
264 generate F1 progeny lacking *Sirt1* expression in the fat body. The progeny received 50% of their
265 genome from the maternal donor strain and 50% from the paternal DGRP strain (Figure S4B).
266 Therefore, we are measuring the dominant effect of the DGRP background on the *Sirt1* RNAi
267 hyperglycemia phenotype. This experimental design is similar to a model of *NGLY1* deficiency
268 using RNAi that was also crossed to the DGRP (Talsness *et al.* 2020).
269
270 In the prior study characterizing the impact of the loss of function of *Sirt1* on metabolic
271 homeostasis, the dysfunction observed was progressive in nature. While larvae and young
272 adults are immediately obese, hyperglycemia and insulin resistance set in and become worse
273 with increasing age (Reis *et al.* 2010; Palu and Thummel 2016). To ensure an appropriate set of
274 conditions with respect to diet and age, we performed a preliminary analysis on 37 DGRP
275 strains at one or two weeks of age, and under fasted or ad libitum fed conditions (Table S1).
276 These time points correspond to conditions in the original study where differences in the
277 metabolic state of the flies corresponded to differences in glycemia (Palu and Thummel 2016).
278 We wished to select a time point at which hyperglycemia was detectable, but also differed
279 enough between strains to allow us to identify genetic variation associated with that
280 heterogeneity.
281
282 Three samples were collected for glucose measurements in each strain and condition. Glucose
283 levels vary across genetic background for each of the conditions being tested (Figure 1A-D).
284 Average glucose for each strain is significantly correlated between one and two week fasted
285 flies (R = 0.53, P = 4E-03), between one-week-old fed and fasted flies (R = 0.45, P = 0.020),
286 and between one-week-old fed and two-week-old fasted flies (R = 0.62, P = 2E-04) (Figure

287 S5A-C). This supports glucose concentration as a consistent quantitative measurement.
288 Interestingly, evidence for correlation with two-week-old flies fed ad libitum is not as strong.
289 While a significant correlation is still detected with one-week-old fasted flies (R = 0.43, P =
290 0.014), the correlation is not significant with two-week-old fasted flies (R = 0.25, P = 0.219) and
291 one-week-old flies fed ad libitum (R = 0.34, P = 0.063) (Figure S5D-F). By two weeks of age,
292 *Sirt1* loss-of-function flies are beginning to experience more severe symptoms of disease, and
293 we expect to see variability in symptoms and behavior in response to those symptoms. Fed flies
294 at two weeks may have more variable glucose because feeding behavior is a big contributor to
295 glucose levels in flies that have not been subjected to a fast.
296
297 To identify the conditions under which the impact of genetic background was the strongest, we
298 performed a one-way ANOVA test that included all data points collected. We found that while
299 there is a significant association between glucose levels and genetic background under all
300 conditions ($p<0.05$), this effect is most pronounced in the one-week-old flies fed ad libitum (P =
301 1.87E-5) and in the two-week-old fasted flies (P = 1.95E-5) (Figure 1A,D). Because fasting
302 reduces possible intra-strain variation caused by food in the gut, two weeks fasted was selected
303 for the full screen.
304
305 We examined protein concentrations in 90 samples from the first 30 strains collected at 2 weeks
306 fasted to ensure that any variation we observe in glucose is not due to differences in body size.
307 Protein levels do not significantly vary across the DGRP (P = 0.63, Figure S6A), nor do protein
308 levels correlate with glucose levels in individual samples (R = 0.04, P = 0.6577, Figure S6B).
309 We conclude that the variation we observe in fasting glucose levels are due to differences in
310 circulating glucose, and not to differences in body size.
311

312 *Genome-wide association analysis identifies candidate modifiers of Sirt1i-associated*
313 *hyperglycemia*
314 Using the conditions determined in the preliminary screen, we proceeded to cross the donor
315 strain with the remaining 149 DGRP strains (Figure 2, Tables S2,S3). We found a significant
316 effect of genetic background on glycemia in the R4>Sirt1i flies (P < 2E-16) using one-way
317 ANOVA including all data points for each strain (N = 555). Individual glucose measurements
318 ranged from 0.306 µg/fly to 3.416 µg/fly (Table S2), while average concentrations ranged from
319 0.395 µg/fly (RAL 801) to 2.438 µg/fly (RAL 357) (Figure 2, Table S3).
320
321 To identify genetic polymorphisms that may be responsible for this observed variation in
322 glycemia, we performed a genome-wide association analysis. Average glucose level for each
323 strain was used as a quantitative phenotype to test for association with polymorphisms in the
324 DGRP. A total of 3,636,891 variants were tested for the *R4>Sirt1i* model across 186 lines. This
325 analysis as a result is insufficiently powered for candidates to remain statistically significant after
326 multiple testing corrections. Instead, the focus is on identification of candidate modifiers and
327 pathways that can be validated through further study and that will provide the basis for future
328 projects. This approach has been quite successful in previous studies (Chow *et al.* 2013, 2015,
329 2016; Palu and Chow 2018; Lavoy *et al.* 2018; Palu *et al.* 2019, 2020; Talsness *et al.* 2020).
330
331 Because the analyzed F1 hybrids in this case were male and inherited their X chromosome from
332 the donor strain and not the DGRP strain, we do not include any X-linked variants in the
333 resulting candidate modifiers. Using an arbitrary cut-off of $P < 10^{-4}$, we identified 237
334 polymorphisms on the second and third chromosomes (Table S4). Of these 237, 62 were not
335 considered further as they were not within +/- 1 kb of a candidate gene. The remaining 175
336 polymorphisms are associated with a total of 161 candidate genes (Table S5). 100 of these
337 polymorphisms are intronic, 29 are exonic with 6 producing non-synonymous changes to the

338 peptide and one a start-gain, 10 are located in the 5' or 3' untranslated regions, and 36 are
339 within 1 kb up or downstream of the candidate gene (Table S4). Of note in this analysis is that
340 the results were not filtered for allele frequency > 0.05. This was a concerted choice; several of
341 the most interesting candidates, including *CG5888* and *ilp5*, would otherwise have been left out
342 of the analysis. The number of total variants analyzed drops from 237 to 90, and the number of
343 candidate genes associated at $P < 10^{-4}$ drops from 161 to 75. While this, along with the use of a
344 low stringency p-value cut-off, increases the probability of false positives, it likewise increases
345 our power when performing pathway enrichment. Validation of candidate genes with low minor
346 allele frequencies in later studies will distinguish true positives from false positives.
347
348 One concern with using an RNAi model to reduce *Sirt1* expression is that the modifiers
349 identified might be specific RNAi efficacy, rather than hyperglycemia. The modifiers could be
350 altering the degree and efficiency of *Sirt1* knockdown, so that hyperglycemia is actually
351 correlating with the amount of *Sirt1* expression that is achieved. If this were the case, we would
352 expect to see the top candidate modifiers associated with RNAi machinery or the efficiency of
353 the GAL4/UAS system. This does not appear to be the case, either from a single-gene function
354 perspective or when looking at enriched gene categories (Tables S5 and S6). Furthermore, the
355 GAL4/UAS system is commonly used to model disease in the DGRP, and the candidates
356 identified have always been unique to the disease and, at times, even the specific model in
357 question (He *et al.* 2014; Chow *et al.* 2016; Lavoy *et al.* 2018; Palu *et al.* 2019; Talsness *et al.*
358 2020). All of this suggests that the candidate genes identified through this screen are modifying
359 *Sirt1*-associated hyperglycemia directly rather than altering the degree of *Sirt1* knockdown.
360
361 *Candidate modifiers of Sirt1 are involved in basic metabolic processes, the immune response,*
362 *and the regulation of neuronal communication*

363 Because loss of *Sirt1* in the fat body alters glucose metabolism and insulin sensitivity in the
364 organism, we expected modifiers of hyperglycemia to impact pathways linked to central carbon
365 metabolism as well as external processes that influence secretion and signaling of hormones
366 such as insulin. To determine if this is the case, we examined the individual functions of the top
367 GWA candidates and looked for pathways and processes that are enriched in this list. While we
368 attempted first to do this through Gene Ontology analysis of our top candidates, we found no
369 significantly enriched terms. We therefore utilized individual known physical interactions and GO
370 term enrichment through GSEA to highlight likely candidate pathways.
371
372 **Analysis of Candidate Modifiers:** We expected our top candidates to include genes that
373 function in pathways or processes related to *Sirt1* regulation or activity. Among the most
374 interesting candidates are those involved in NAD metabolism. We identified two genes whose
375 products are part of the NADH dehydrogenase component of Complex I in the electron transport
376 chain (*NDUFS3* and *ND-PDSW*) (FlyBase Curators 2008; Gaudet *et al.* 2011). There are also
377 two NADP kinases, enzymes involved in the generation of NADP from NAD (*CG33156* and
378 *CG6145*) (Gaudet *et al.* 2011). *DUOX*, an NADPH oxidase, passes electrons from NADPH to
379 oxygen, generating hydrogen peroxide and altering the redox balance of the cell (Gaudet *et al.*
380 2011; Anh *et al.* 2011). As Sirt1 utilizes NAD as a cofactor during its enzymatic reaction, altering
381 the balance of NAD in the cell through differential regulation of these enzymes could further
382 impact the activity of other pathways that require NAD as an electron carrier, or exacerbate the
383 phenotypes associated with *Sirt1* loss-of function (Nogueiras *et al.* 2012). We also identified two
384 genes that have previously been implicated in the regulation and/or extension of lifespan: *sugb*
385 and *CG42663* (Landis *et al.* 2003; Paik *et al.* 2012). While the role of *Sirt1* in lifespan extension
386 is still contested, the identification of other genes implicated in this process suggests shared
387 functions or pathways.
388

389 Genes involved in central glucose metabolism as well as insulin signaling are also candidate
390 modifiers. MFS5 acts as a transporter of both glucose and trehalose for the uptake of these
391 sugars from circulation (McMullen *et al.* 2021). Glucose-6-phosphatase (*G6P*) is the last rate-
392 limiting step in both gluconeogenesis and glycogenolysis, which are used to generate glucose
393 for release into the body during fasting (Gaudet *et al.* 2011; Lizák *et al.* 2019). These two genes
394 directly regulate circulating glucose levels. Candidates involved in other metabolic pathways
395 include *CTPSyn*, which encodes the rate limiting step in cytidine synthesis, the very long chain
396 fatty acid ligase *bgm*, the mannosidase *Edem2*, and the oxoglutarate dehydrogenase complex
397 subunit *CG33791* (Kang and Ryoo 2009; Gaudet *et al.* 2011; Jang *et al.* 2015; Sivachenko *et al.*
398 2016; Zhou *et al.* 2019). Partially responsible for regulating general metabolic flux through these
399 various pathways is insulin. Interestingly, a top candidate is *ilp5*, one of several insulin-like
400 peptides expressed in the insulin-producing cells (IPCs) in the *Drosophila* brain (Géminard *et al.*
401 2009). Our analysis also identified *IA-2*, a phosphatase involved in ilp secretion, *CG4168*, an
402 uncharacterized gene whose closest human orthologue *IGFALS* encodes a protein that binds to
403 and stabilizes IGF proteins in circulation, and *wrd*, a subunit in the protein phosphatase PP2A
404 that negatively regulates insulin and TOR signaling (Boisclair *et al.* 1996; Kim *et al.* 2008; Hahn
405 *et al.* 2010).
406
407 Other potential modifiers of insulin stability and signaling in circulation are *dally*, *cow*, and *Hs3st-*
408 *A*. Both *dally* and *cow* encode heparin sulfate proteoglycans, while *Hs3st-A* encodes an O-
409 sulfotransferase that acts on these proteoglycans (Filmus and Selleck 2001; Gaudet *et al.* 2011;
410 Chang and Sun 2014). Previous work has demonstrated an impact of the enzyme heparanase,
411 which cleaves heparan sulfate, on diabetic autoimmunity and complications such as
412 nephropathy (Rabelink *et al.* 2017). While this is more peripheral to the central insulin signaling
413 pathway in *Drosophila*, it highlights the utility of such factors in altering disease processes in
414 subtle ways.

415

416 Another interesting group of candidates are those associated with neuronal development and
417 function. Several members of the defective proboscis extension response (*dpr*) family were
418 represented in our list (*dpr2*, *dpr6*, and *dpr13*) along with the dpr-interacting protein *DIP-eta*.
419 The *dpr* gene family is collectively associated with synapse organization and function, as are the
420 candidate genes *fife*, *CG32373*, and *atilla* (FlyBase Curators *et al.* 2004; Kurusu *et al.* 2008;
421 Carrillo *et al.* 2015; Bruckner *et al.* 2017). We also noted candidates involved in neuropeptide
422 signaling (*rk* and *RYa-R*), voltage-gated potassium channels and their regulation (*CG5888* and
423 *CG1688*), and axon guidance (*tutl*, *CadN2*, *CG34353*, and *sbb*) (Rao *et al.* 2000; Luo *et al.*
424 2005; Prakash *et al.* 2005; Al-Anzi and Wyman 2009; Ida *et al.* 2011; Gaudet *et al.* 2011). The
425 IPCs in *Drosophila* are actually neuroendocrine cells located in the brain, as are the AKH-
426 producing cells responsible for secreting the glucagon-like hormone AKH (Géminard *et al.*
427 2006). The secretion of insulin is therefore dependent upon the correct development,
428 connection, and signaling of neuronal cells.

429

430 The immune response is another generally enriched category of modifier genes. Several
431 members of the nimrod family of immunoglobulins (*NimB2*, *NimC1*, and *NimC3*) were identified
432 by GWA. All are implicated in the innate immune response, with *NimC1* and *NimC3* in particular
433 having roles in phagocytosis (Somogyi *et al.* 2010). In response to insecticides, *LRR* regulates
434 the immune response through NF-kappaB, whose activation is an early protective event in the
435 progression and pathology of diabetes (Prisco *et al.* 2013; Irvin *et al.* 2018). Two lysozyme
436 enzymes with links to bacterial defense (*LysX* and *CG7798*) highlight the role of oxidative stress
437 and redox homeostasis in the innate immune response (FlyBase Curators 2008). As Sirt1 has
438 roles in regulating the response to oxidative stress, we looked for other genes with similar
439 functions (Brunet *et al.* 2004). As described above, *DUOX* plays a part in regulating redox
440 homeostasis through the production of hydrogen peroxide (Anh *et al.* 2011). *CG42331* encodes

441 a peroxidase that appears to be strongly enriched in the pupal fat body, and *cyp28a5* encodes
442 an oxidoreductase that, similar to LRR, is involved in the response to insecticides (FlyBase
443 Curators *et al.* 2004; Graveley *et al.* 2011; Gaudet *et al.* 2011). It is now believed that Type I
444 and Type II diabetics both suffer at least to some degree from autoimmunity (Candia *et al.*
445 2019). Exploring the direct and indirect connections of *Sirt1* to the immune response and
446 oxidative stress directly is an interesting avenue for future direction.
447
448 **Physical Interaction Network:** We generated a network of physical interactions among the 161
449 candidate genes identified above. These were identified and visualized using Cytoscape
450 software with the GeneMania plugin (Shannon *et al.* 2003; Montojo *et al.* 2010). The products of
451 37/161 candidate genes were found to physically interact with at least one other candidate gene
452 product with no more than one bridging node represented by a non-candidate gene (Figure 3A).
453 This high degree of interaction suggests that the modifiers identified in this screen are indeed
454 functioning through shared processes.
455
456 Focusing then on the 37 genes involved in physical interactions, we identified several broad
457 functional categories that could influence glucose homeostasis in the fly. The most obvious
458 category are enzymes that catalyze steps in basic metabolic pathways (N = 7). This includes
459 the NAD kinases (*CG6145* and *CG33156*) and one NADH dehydrogenase (*ND-PDSW*)
460 discussed above (Gaudet *et al.* 2011). Other metabolic candidate modifiers include *MFS3* and
461 *CTPsyn*, the rate limiting enzyme in the production of the nucleotide Cytidine triphosphate (Zhou
462 *et al.* 2019). Both of these enzymes function in pathways critically dependent upon or feeding
463 into central carbon metabolism, and their inclusion as candidate modifiers of hyperglycemia
464 supports a role for those secondary metabolic pathways as a sink for increased circulating
465 glucose. *Mtmr6* encodes a phosphatidylinositol phosphatase, a key enzyme in several signaling
466 pathways, including insulin signaling (Gaudet *et al.* 2011). Also interesting is the gene *LRP1*,

467 which is orthologous to human LDL receptor related protein 1. In additional to its role in lipid
468 homeostasis, *LRP1* has also been implicated in Alzheimer's disease, for which metabolic
469 disease and obesity are risk factors (Kang *et al.* 2000; Anstey *et al.* 2011).
470
471 Curiously, several of the genes highlighted in this analysis also happen to localize specifically to
472 the mitochondria (N = 4). *Roe1* and *porin* are both transporters involved in the import of
473 molecules into the mitochondria (Komarov *et al.* 2004; Jana Alonso *et al.* 2005; FlyBase
474 Curators 2008; Gaudet *et al.* 2011). The NADH dehydrogenases *ND-PDSW* and *NDUFS3* both
475 function in the mitochondria as well as part of Complex I in the electron transport chain
476 (Jana Alonso *et al.* 2005). Closer examination of the top GWA candidates reveals additional
477 mitochondrial localization candidates including the amino acyl tRNA synthetase *GlyRS*, the
478 membrane bound regulator of protein kinase A (*pkaap*) and the translation elongation factor
479 *mEFTu1* (Gaudet *et al.* 2011; Lu *et al.* 2016). In adult metabolic homeostasis, central carbon
480 metabolism is generally used to fuel the electron transport chain in the mitochondria and
481 generate ATP for the cell (Barry and Thummel 2016). Altering the activity of this essential
482 downstream pathway could have a clear impact on glucose utilization and disease progression
483 in diabetes.
484
485 Similar to our examination of top candidates, our physical interaction map highlighted the
486 immune response (*NimC1*, *NimC3*, *NimB2*, and *LRR*) and neuronal function. *Tutl*, *dpr2*, and
487 *DIP-eta,* and *wb* are all involved in synapse organization and axon guidance, while *Pax* and
488 *rhea* are involved in focal adhesion (Delon and Brown 2009). The identification of genes
489 important for cellular communication suggests that some of the modifiers identified in this study
490 have roles in tissues other than the fat body, such as the IPC and APC neurons. This is an
491 important avenue of future exploration.
492

493 **Gene Set Enrichment Analysis (GSEA):** In the second approach, we performed GSEA
494 analysis to identify gene ontology terms for which associated variants are enriched. Unlike
495 traditional GO analysis, which relies upon a set of genes based on a P-value cutoff, GSEA
496 examines the entire gene set (Dyer *et al.* 2008). For each defined GO category, GSEA
497 determines whether the members of that category are randomly distributed throughout the
498 ranked gene list provided or if they are enriched for the lower p-values found at the top of that
499 list. GO categories enriched at the top of the list describe important functions of the gene set.
500 GSEA identified 52 significantly associated gene sets (≥ 3 genes) with positive enrichment
501 scores at a p-value of <0.05 (Table S6, Figure 3B). The top two gene sets implicate neuronal
502 function and communication in the *Sirt1i*-associated hyperglycemia phenotype: calcium-
503 activated potassium channel activity (GO:0015269, P = 1.1E-3) and maintenance of presynaptic
504 active zone structure (GO:0048790, P = 1.2E-3). Similar categories can be found through the
505 list of significantly associated gene sets, including dendrite morphogenesis (GO:0048813, P =
506 0.049), which represents the largest group of genes at N = 119 and contains two of the top
507 GWA candidates (*slit* and *fruitless*). Coupled with the neuronal genes identified in our physical
508 interaction network, this suggests that function in the neuroendocrine cells could play a big role
509 in glucose homeostasis in the fat body.
510
511 Also enriched are taste receptor activity (GO:0008527, P = 0.013) and sensory reception of
512 taste (GO:0050909, P = 0.018). These categories highlight a yet unconsidered factor that must
513 be taken into account with metabolic phenotypes: that of feeding and diet. While all flies were
514 collected under identical conditions and were maintained on the same diet, it is nonetheless
515 possible that some may simply be eating more due to differences in the sensing of satiation or
516 to differences in perception of taste. These differences in perception and consumption can have
517 detectable impacts on metabolic phenotypes (May *et al.* 2019).
518

519 As expected, we also see evidence of general metabolic processes. Some, like alpha,alpha-
520 trehalase activity (GO:0004555, P = 0.043) and phosphatidylinositol transporter activity
521 (GO:0008526, P = 0.013) have direct links to glucose metabolism and insulin signaling. Others,
522 such as oxysterol binding (GO:0008142, P = 0.026), glutamate biosynthetic process
523 (GO:0006537, P = 0.043), and isoprenoid biosynthetic process (GO:0008299, P = 0.048)
524 function more peripherally to carbon metabolism and are likely influencing hyperglycemia by
525 their general contribution to physiological homeostasis.
526
527 Another interesting group of GO categories highlighted by GSEA are RNA processing functions.
528 rRNA (uridine-2'-O-)-methyltransferase activity (GO:0008650, P = 2.4E-3) is the fourth most
529 associated category as ranked by p-value, and others such as snoRNA binding (GO:0030515, P
530 = 0.014) reiterating this function. The presence of RNA processing categories is of particular
531 interest because three of the top candidate genes by GWA are splicing factors (*bru1*, *fand*, and
532 *snRNP-U1-70k*) (Park *et al.* 2004; Oas *et al.* 2014; Spletter *et al.* 2015). While it is unclear how
533 rRNA or mRNA processing may directly or indirectly influence glucose homeostasis in
534 particular, the identification of this process through several different methods of analysis is
535 striking and worth further exploration.
536
537 *Functional analysis of candidate modifier genes*
538 To confirm the roles of our candidate genes in regulating glucose homeostasis, we elected to
539 test the impact of loss of modifier expression for 16 of the most significant candidates for which
540 we were able to obtain transgenic RNAi lines (Table 1). We crossed the RNAi strains targeting
541 each of these modifiers into the *R4>Sirt1i* line, aged the resulting progeny for 2-3 weeks, and
542 measured glucose in fasted males. We also measured protein levels as a control. Knockdown of
543 modifier genes did not significantly alter protein levels as compared to a genetically matched
544 control (Figure S7). Knockdown of the genes *CG4168*, *CG5888*, and *uif* resulted in suppression

545 of the hyperglycemia phenotype, with a significant decrease in glucose content per fly compared
546 to controls expressing *R4>Sirt1i* (Figure 4). These results demonstrate that many of the top
547 GWA candidate modifiers are capable of modifying the hyperglycemia phenotypes associated
548 with the *R4>Sirt1i* model of diabetes.
549

550 **DISCUSSION**

551 Identifying and characterizing the genetic factors influencing the severity of diabetes is critical to
552 early diagnosis. Prevention is still the best strategy available, and providing patients at high risk
553 for complications with knowledge of that risk could prevent the worst symptoms from
554 manifesting. It could even enable intervention before the progression of disease is irreversible.
555

556 In this study, we identified and analyzed a number of candidate modifiers of hyperglycemia in a
557 previously characterized model of diabetes, *Sirt1* loss-of-function. We used the DGRP as an
558 unbiased source of natural genetic variation for this screen. This is the first time a genetic model
559 of metabolic dysfunction has been put to this use, as previous screens have either focused on
560 dietary stress as a source of metabolic disease or on the impact of genotype on metabolic
561 parameters under non-stressed conditions (Mackay *et al.* 2012; Ivanov *et al.* 2015; Nelson *et al.*
562 2016; Jehrke *et al.* 2018; Everman *et al.* 2019). We observed very little overlap in modifier
563 candidates between our observations and these studies. This is consistent with previous work
564 demonstrating that even when the observed phenotypes are similar or nearly identical, the
565 overlap in modifiers is often small in different models of disease (Palu *et al.* 2019). One
566 exception is a screen for the response to starvation resistance performed by Everman *et al.* in
567 2018. They identified *CG15803*, a transporter of unknown function that was also identified in our
568 studies (Everman and Morgan 2018). While our preliminary analysis suggests that this gene
569 does not function in the fat body, it is possible that it could have a role in another physiologically
570 relevant tissue such as the IPCs or APCs. Indeed, *CG15803* appears to be most highly

571 expressed in the head and CNS (Graveley *et al.* 2011). This is an interesting avenue of future
572 exploration.
573
574 We did observe overlap in general gene categories with previous studies, even when direct
575 overlaps were few. This was found to be true for modifiers of neuronal function. In a broad
576 exploration of genetic variation in the nutrient response that looked at triglycerides, starvation
577 resistance, mass, and glucose, *NimB3* was identified as a candidate modifier (Nelson *et al.*
578 2016). While *NimB3* was not identified in this screen, we did find *NimB2*, *NimC1*, and *NimC3*.
579 *Fife*, which also has roles in synapse organization, was identified in this study and one for
580 starvation resistance (Mackay *et al.* 2012). As mentioned above, both the IPCs and APCs are
581 neuroendocrine cells found in or near the brain (Géminard *et al.* 2006). Maintenance of neuronal
582 function would be critical to hormonal balance as a result. Furthermore, it is broadly
583 acknowledged that metabolic homeostasis is also dependent upon feeding rate, over which the
584 central nervous system has some sway (Owusu-Ansah and Perrimon 2014). The identification
585 of neuronal genes in each analysis suggests that regulation of particular neuronal pathways and
586 cells is critical to the maintenance of physiological homeostasis.
587
588 Given the prevalence of neuronal and sensory perception genes in the analysis, a concern
589 could be raised for the role feeding rate could be playing in the variation of glucose across the
590 DGRP. To assess this, we compared glucose with male feeding rate in a previous analysis
591 (Table S3) (Garlapow *et al.* 2015). We saw no correlation whatsoever, indicating that while
592 nutrient sensing may play a role in the response to Sirt1i-induced hyperglycemia, it is not the
593 driving factor in the variation observed in this screen (Figure S8).
594
595 Another interesting category highlighted through several analysis methods is the innate immune
596 response. While it has long been known that Type I diabetes is an autoimmune disorder, it has

597 recently been acknowledged that Type II diabetics also display symptoms of autoimmunity
598 (Candia *et al.* 2019). Furthermore, insulin resistance has frequently been associated with
599 inflammation, and the presence of macrophages in the adipose tissue is a hallmark of obesity
600 and diabetes (Wu and Ballantyne 2020). Modifiers associated with innate immunity serve
601 therefore as validation to the study as a whole, and examination of these genes and their
602 function in the context of the *Sirt1* loss-of-function model will be an intriguing focus of future
603 research.
604
605 An important component of this study is the validation of top candidate modifiers using RNAi-
606 mediated knockdown of gene expression. We obtained strains expression transgenic RNAi
607 constructs targeting 16 of the most significant candidates (Table 1). We found that reduced
608 expression of three candidates specifically in the fat body resulted in significant suppression of
609 hyperglycemia: *CG4168*, *CG5888*, and *uif* (Figure 4). We also noted a consistent, though not
610 significant, decrease in glucose for two independent RNAi constructs targeting *CTPSyn*,
611 suggesting that this gene warrants further study (Figure 4, data not shown). The remainder of
612 the genes had no significant or consistent impact on hyperglycemia in the model of *Sirt1* loss-of-
613 function (Figure 4). There were no enhancing modifiers: loss of modifier expression did not lead
614 to increased glucose levels for any of the tested genes. This could be because hyperglycemia is
615 already quite strong in the *Sirt1* loss-of-function model, or because we simply did not hit on any
616 enhancing modifiers. Of greater concern is the lack of any response for 13 of the 16 tested
617 candidates. One explanation may be found in the large number of known neuronal genes
618 identified in this analysis. This modifier RNAi screen specifically focused on the expression of
619 the RNAi against the candidate genes in the fat body, where expression of *Sirt1* is also reduced.
620 If, however, the function of a modifier gene is primarily concentrated in the IPCs, as with *ilp5*,
621 reducing its expression in the fat body would have little effect on the disease phenotypes in

622 question. We will examine the role of modifier genes not only in the fat body but in the IPCs,
623 APCs, and other physiologically relevant tissues in future work.
624
625 Of immediate interest is of course the mechanism of action for the three suppressor genes that
626 were confirmed by RNAi in the fat body. Of these, *CG5888* is also the top GWA candidate (P =
627 2.80E-07). While largely uncharacterized, *CG5888* has been identified as a component or
628 activator of voltage-gated potassium channels by sequence homology (Gaudet *et al.* 2011).
629 Intriguingly, it has also been implicated JNK signaling by a previous RNAi screen (Bond and
630 Foley 2009). JNK signaling is commonly activated by cellular stress and can activate apoptosis.
631 It also has important roles in the signaling pathways commonly used by the immune system
632 (Bond and Foley 2009; Shlevkov and Morata 2012). A potential role for *CG5888* in immune
633 pathways has yet to be explored and could be an exciting area of further discovery.
634
635 *Uninflatable* (*uif*) encodes a single pass transmembrane protein found on the apical membrane
636 of epithelial cells and has been found to enable Notch signaling (Loubéry *et al.* 2014). It has
637 also been found to exacerbate disease in a *Drosophila* model of muscular dystrophy
638 (Kucherenko *et al.* 2011), and its closest human orthologue ELAPOR1 is a regulator of
639 apoptosis and autophagy (Deng *et al.* 2010). Both of these processes are commonly disrupted
640 through inappropriate activation in metabolic disease, and might provide some explanation for
641 the impact of *uif* on *Sirt1i*-associated phenotypes (Bugliani *et al.* 2019).
642
643 Perhaps the most intriguing finding is *CG4168* as the modifier with the strongest impact on
644 *Sirt1i*-associated hyperglycemia. The protein encoded by *CG4168* is of unknown function, but
645 its closest human orthologue (*IGFALS*) encodes a serum protein that binds to insulin-like growth
646 factors (IGF) in circulation (Boisclair *et al.* 1996). In mammals, association with IGFALS
647 increases the half-life of insulin-like growth factors in the serum as well as their retention in

648 circulation. While studies of IGFALS in mammals has not shown a role for it in regulating insulin
649 signaling, the *Drosophila* ilp peptides are used for both IGF and insulin signaling activation
650 (Géminard *et al.* 2006). It is possible that secretion of the factor encoded by *CG4168* from the
651 fat body could increase ilp retention in circulation, whereas its loss could result in faster
652 clearance of ilps from circulation. Under conditions that promote insulin resistance, such as the
653 loss of *Sirt1*, it is possible that reduced ilp levels in the hemolymph could slow or prevent insulin
654 resistance and hyperglycemia. Further exploration of the mechanisms behind the action of
655 *CG4168* could reveal important insights into circulating insulin-binding factors and their role in
656 diabetes.
657
658 In conclusion, we have identified a number of pathways and processes involved in the degree of
659 hyperglycemia in a genetic model of diabetes. Examination of the candidate genes and
660 pathways described above in this model as well as other models of metabolic dysfunction will
661 shed new light on the mechanism by which insulin resistance and related complications disease
662 onset, progression, and severity. Furthermore, the candidates identified as suppressors could
663 serve as promising targets for therapeutics in diabetes and related metabolic disorders.
664

665 **DATA AVAILABILITY STATEMENT**

666 Strains and stocks are available upon request, as is code for GSEA. Genomic sequence for the
667 DGRP is available at http://dgrp.gnets.ncsu.edu/. Supplemental material is available at FigShare
668 (https://figshare.com/s/2b0b0237de0f94139a4f).
669

670 **ACKNOWLEDGEMENTS**

671 We thank Katie G. Owings and Clement Y. Chow for their contributions to the data analysis in
672 this project, as well as reagents and comments. This research was supported by a Faculty

673 Summer Research Grant through the Purdue University-Fort Wayne Office of Sponsored
674 Projects to RASP as well as the Purdue University-Fort Wayne Department of Biology.
675

676 **REFERENCES**

677 Al-Anzi B., and R. J. Wyman, 2009 The Drosophila immunoglobulin gene turtle encodes
678 guidance molecules involved in axon pathfinding. Neural Dev. 2009 41 4: 1–15.
679 https://doi.org/10.1186/1749-8104-4-31
680 Anh N. T. T., M. Nishitani, S. Harada, M. Yamaguchi, and K. Kamei, 2011 Essential Role of
681 Duox in Stabilization of Drosophila Wing. J. Biol. Chem. 286: 33244–33251.
682 https://doi.org/10.1074/JBC.M111.263178
683 Anstey K. J., N. Cherbuin, M. Budge, and J. Young, 2011 Body mass index in midlife and late-
684 life as a risk factor for dementia: a meta-analysis of prospective studies. Obes. Rev. 12:
685 e426–e437. https://doi.org/10.1111/J.1467-789X.2010.00825.X
686 Arrese E. L., and J. L. Soulages, 2010 Insect Fat Body: Energy, Metabolism, and Regulation.
687 Annu. Rev. Entomol. 55: 207–225. https://doi.org/10.1146/annurev-ento-112408-085356
688 Barroso I., and M. I. McCarthy, 2019 The Genetic Basis of Metabolic Disease. Cell 177: 146–
689 161. https://doi.org/10.1016/j.cell.2019.02.024
690 Barry W. E., and C. S. Thummel, 2016 The Drosophila HNF4 nuclear receptor promotes
691 glucose-stimulated insulin secretion and mitochondrial function in adults. Elife 5.
692 https://doi.org/10.7554/ELIFE.11183
693 Beebe K., M. M. Robins, E. J. Hernandez, G. Lam, M. A. Horner, *et al.*, 2020 Drosophila
694 estrogen-related receptor directs a transcriptional switch that supports adult glycolysis and
695 lipogenesis. Genes Dev. 34: 701. https://doi.org/10.1101/GAD.335281.119
696 Biason-Lauber A., M. Böni-Schnetzler, B. P. Hubbard, K. Bouzakri, A. Brunner, *et al.*, 2013
697 Identification of a SIRT1 Mutation in a Family with Type 1 Diabetes. Cell Metab. 17: 448–
698 455. https://doi.org/10.1016/J.CMET.2013.02.001

699 Boisclair Y. R., D. Seto, S. Hsieh, K. R. Hurst, and G. T. Ooi, 1996 Organization and
700 chromosomal localization of the gene encoding the mouse acid labile subunit of the insulin-
701 like growth factor binding complex. Proc. Natl. Acad. Sci. 93: 10028–10033.
702 https://doi.org/10.1073/PNAS.93.19.10028
703 Bond D., and E. Foley, 2009 A quantitative RNAi screen for JNK modifiers identifies Pvr as a
704 novel regulator of Drosophila immune signaling. PLoS Pathog. 5.
705 https://doi.org/10.1371/JOURNAL.PPAT.1000655
706 Botden I. P. G., M. C. Zillikens, S. R. de Rooij, J. G. Langendonk, A. H. J. Danser, *et al.*, 2012
707 Variants in the SIRT1 Gene May Affect Diabetes Risk in Interaction With Prenatal
708 Exposure to Famine. Diabetes Care 35: 424–426. https://doi.org/10.2337/DC11-1203
709 Boutant M., and C. Cantó, 2014 SIRT1 metabolic actions: Integrating recent advances from
710 mouse models. Mol. Metab. 3: 5–18.
711 Bruckner J. J., H. Zhan, S. J. Gratz, M. Rao, F. Ukken, *et al.*, 2017 Fife organizes synaptic
712 vesicles and calcium channels for high-probability neurotransmitter release. J. Cell Biol.
713 216: 231–246. https://doi.org/10.1083/JCB.201601098
714 Brunet A., L. Sweeney, J. Sturgill, K. Chua, P. Greer, *et al.*, 2004 Stress-dependent regulation
715 of FOXO transcription factors by the SIRT1 deacetylase. Science 303: 2011–2015.
716 https://doi.org/10.1126/SCIENCE.1094637
717 Bugliani M., S. Mossuto, F. Grano, M. Suleiman, L. Marselli, *et al.*, 2019 Modulation of
718 Autophagy Influences the Function and Survival of Human Pancreatic Beta Cells Under
719 Endoplasmic Reticulum Stress Conditions and in Type 2 Diabetes. Front. Endocrinol.
720 (Lausanne). 10: 52. https://doi.org/10.3389/fendo.2019.00052
721 Cabrera A. P., R. N. Mankad, L. Marek, R. Das, S. Rangasamy, *et al.*, 2020 Genotypes and
722 Phenotypes: A Search for Influential Genes in Diabetic Retinopathy. Int. J. Mol. Sci. 2020,
723 Vol. 21, Page 2712 21: 2712. https://doi.org/10.3390/IJMS21082712
724 Candia P. de, F. Prattichizzo, S. Garavelli, V. De Rosa, M. Galgani, *et al.*, 2019 Type 2

725 Diabetes: How Much of an Autoimmune Disease? Front. Endocrinol. (Lausanne). 10: 451.
726 https://doi.org/10.3389/FENDO.2019.00451
727 Carrillo R. A., E. Özkan, K. P. Menon, S. Nagarkar-Jaiswal, P.-T. Lee, *et al.*, 2015 Control of
728 Synaptic Connectivity by a Network of Drosophila IgSF Cell Surface Proteins. Cell 163:
729 1770–1782. https://doi.org/10.1016/J.CELL.2015.11.022
730 CDC, 2020 National Diabetes Statistics Report 2020. Estimates of diabetes and its burden in
731 the United States.
732 Chang Y.-H., and Y. H. Sun, 2014 Carrier of Wingless (Cow), a Secreted Heparan Sulfate
733 Proteoglycan, Promotes Extracellular Transport of Wingless. PLoS One 9: e111573.
734 https://doi.org/10.1371/JOURNAL.PONE.0111573
735 Chow C. Y., M. F. Wolfner, and A. G. Clark, 2013 Using natural variation in Drosophila to
736 discover previously unknown endoplasmic reticulum stress genes. Proc Natl Acad Sci U S
737 A 110: 9013–9018. https://doi.org/10.1073/pnas.1307125110
738 Chow C. Y., F. W. Avila, A. G. Clark, and M. F. Wolfner, 2015 Induction of excessive
739 Endoplasmic reticulum stress in the Drosophila male accessory gland results in infertility.
740 PLoS One 10: 1–12. https://doi.org/10.1371/journal.pone.0119386
741 Chow C. Y., 2016 Bringing genetic background into focus. Nat. Rev. Genet. 17: 63–64.
742 https://doi.org/10.1038/nrg.2015.9
743 Chow C. Y., K. J. P. Kelsey, M. F. Wolfner, and A. G. Clark, 2016 Candidate genetic modifiers
744 of retinitis pigmentosa identified by exploiting natural variation in Drosophila. Hum. Mol.
745 Genet. 25: 651–659. https://doi.org/10.1093/HMG/DDV502
746 Chow C. Y., and L. T. Reiter, 2017 Etiology of Human Genetic Disease on the Fly. Trends
747 Genet. 33: 391–398. https://doi.org/10.1016/j.tig.2017.03.007
748 Delon I., and N. H. Brown, 2009 The integrin adhesion complex changes its composition and
749 function during morphogenesis of an epithelium. J. Cell Sci. 122: 4363–4374.
750 https://doi.org/10.1242/JCS.055996

751 Deng L., J. Feng, and R. R. Broaddus, 2010 The novel estrogen-induced gene EIG121
752 regulates autophagy and promotes cell survival under stress. Cell Death Dis. 1: e32.
753 https://doi.org/10.1038/CDDIS.2010.9
754 DiAngelo J. R., and M. J. Birnbaum, 2009 Regulation of Fat Cell Mass by Insulin in Drosophila
755 melanogaster. Mol. Cell. Biol. 29: 6341–6352. https://doi.org/10.1128/mcb.00675-09
756 Dyer M. D., T. M. Murali, and B. W. Sobral, 2008 The Landscape of Human Proteins Interacting
757 with Viruses and Other Pathogens. PLoS Pathog. 4: e32.
758 https://doi.org/10.1371/journal.ppat.0040032
759 Everman E. R., and T. J. Morgan, 2018 Antagonistic pleiotropy and mutation accumulation
760 contribute to age-related decline in stress response. Evolution (N. Y). 72: 303–317.
761 https://doi.org/10.1111/EVO.13408
762 Everman E. R., C. L. McNeil, J. L. Hackett, C. L. Bain, and S. J. Macdonald, 2019 Dissection of
763 Complex, Fitness-Related Traits in Multiple Drosophila Mapping Populations Offers Insight
764 into the Genetic Control of Stress Resistance. Genetics 211: 1449–1467.
765 https://doi.org/10.1534/genetics.119.301930
766 Filmus J., and S. B. Selleck, 2001 Glypicans: proteoglycans with a surprise. J. Clin. Invest. 108:
767 497–501. https://doi.org/10.1172/JCI13712
768 Flegal K., D. Kruszon-Moran, M. Carroll, C. Fryar, and C. Ogden, 2016 Trends in Obesity
769 Among Adults in the United States, 2005 to 2014. JAMA 315: 2284–2291.
770 https://doi.org/10.1001/JAMA.2016.6458
771 FlyBase Curators, Swiss-Prot Project Members, and InterPro Project Members, 2004 Gene
772 Ontology annotation in FlyBase through association of InterPro records with GO terms.
773 FlyBase Curators, 2008 Assigning Gene Ontology (GO) terms by sequence similarity in
774 FlyBase.
775 Garlapow M. E., W. Huang, M. T. Yarboro, K. R. Peterson, and T. F. C. Mackay, 2015
776 Quantitative Genetics of Food Intake in Drosophila melanogaster. PLoS One 10:

e0138129. https://doi.org/10.1371/JOURNAL.PONE.0138129

Gaudet P., M. S. Livstone, S. E. Lewis, and P. D. Thomas, 2011 Phylogenetic-based propagation of functional annotations within the Gene Ontology consortium. Brief. Bioinform. 12: 449–462. https://doi.org/10.1093/bib/bbr042

Géminard C., N. Arquier, S. Layalle, M. Bourouis, M. Slaidina, *et al.*, 2006 Control of metabolism and growth through insulin-like peptides in Drosophila. Diabetes 55: S5–S8. https://doi.org/10.2337/db06-S001

Géminard C., E. J. Rulifson, and P. Léopold, 2009 Remote Control of Insulin Secretion by Fat Cells in Drosophila. Cell Metab. 10: 199–207. https://doi.org/10.1016/j.cmet.2009.08.002

Graveley B. R., G. May, A. N. Brooks, J. W. Carlson, L. Cherbas, *et al.*, 2011 The D. melanogaster transcriptome: modENCODE RNA-Seq data for dissected tissues

Hahn K., M. Miranda, V. A. Francis, J. Vendrell, A. Zorzano, *et al.*, 2010 PP2A Regulatory Subunit PP2A-B′ Counteracts S6K Phosphorylation. Cell Metab. 11: 438–444. https://doi.org/10.1016/J.CMET.2010.03.015

He B. Z., M. Z. Ludwig, D. A. Dickerson, L. Barse, B. Arun, *et al.*, 2014 Effect of Genetic Variation in a Drosophila Model of Diabetes-Associated Misfolded Human Proinsulin. Genetics 196: 557. https://doi.org/10.1534/GENETICS.113.157800

Huang W., A. Massouras, Y. Inoue, J. Peiffer, M. Ràmia, *et al.*, 2014 Natural variation in genome architecture among 205 Drosophila melanogaster Genetic Reference Panel lines. Genome Res. 24: 1193–208. https://doi.org/10.1101/gr.171546.113

Ida T., T. Takahashi, H. Tominaga, T. Sato, K. Kume, *et al.*, 2011 Identification of the novel bioactive peptides dRYamide-1 and dRYamide-2, ligands for a neuropeptide Y-like receptor in Drosophila. Biochem. Biophys. Res. Commun. 410: 872–877. https://doi.org/10.1016/J.BBRC.2011.06.081

Irvin A. E., G. Jhala, Y. Zhao, T. S. Blackwell, B. Krishnamurthy, *et al.*, 2018 NF-κB is weakly activated in the NOD mouse model of type 1 diabetes. Sci. Reports 2018 81 8: 1–7.

803 https://doi.org/10.1038/s41598-018-22738-3
804 Ivanov D. K., V. Escott-Price, M. Ziehm, M. M. Magwire, T. F. C. Mackay, *et al.*, 2015 Longevity
805 GWAS using the drosophila genetic reference panel. Journals Gerontol. - Ser. A Biol. Sci.
806 Med. Sci. 70: 1470–1478. https://doi.org/10.1093/gerona/glv047
807 Ivy J., A. Klar, and J. Hicks, 1986 Cloning and characterization of four SIR genes of
808 Saccharomyces cerevisiae. Mol. Cell. Biol. 6: 688–702.
809 https://doi.org/10.1128/MCB.6.2.688-702.1986
810 Jana Alonso, Javier M. Rodriguez, and Luis Alberto Baena-López, and J. F. Santarén*, 2005
811 Characterization of the Drosophila melanogaster Mitochondrial Proteome. J. Proteome
812 Res. 4: 1636–1645. https://doi.org/10.1021/PR050130C
813 Jang B.-Y., H. D. Ryoo, J. Son, K.-C. Choi, D.-M. Shin, *et al.*, 2015 Role of Drosophila EDEMs
814 in the degradation of the alpha-1-antitrypsin Z variant. Int. J. Mol. Med. 35: 870–876.
815 https://doi.org/10.3892/IJMM.2015.2109
816 Jehrke L., F. A. Stewart, A. Droste, and M. Beller, 2018 The impact of genome variation and diet
817 on the metabolic phenotype and microbiome composition of Drosophila melanogaster. Sci.
818 Rep. 8. https://doi.org/10.1038/S41598-018-24542-5
819 Kang D. E., C. U. Pietrzik, L. Baum, N. Chevallier, D. E. Merriam, *et al.*, 2000 Modulation of
820 amyloid β-protein clearance and Alzheimer's disease susceptibility by the LDL receptor–
821 related protein pathway. J. Clin. Invest. 106: 1159–1166. https://doi.org/10.1172/JCI11013
822 Kang M.-J., and H. D. Ryoo, 2009 Suppression of retinal degeneration in Drosophila by
823 stimulation of ER-associated degradation. Proc. Natl. Acad. Sci. U. S. A. 106: 17043–8.
824 https://doi.org/10.1073/pnas.0905566106
825 Kim J., H. Bang, S. Ko, I. Jung, H. Hong, *et al.*, 2008 Drosophila ia2 modulates secretion of
826 insulin-like peptide. Comp. Biochem. Physiol. Part A Mol. Integr. Physiol. 151: 180–184.
827 https://doi.org/10.1016/J.CBPA.2008.06.020
828 Komarov A. G., B. H. Graham, W. J. Craigen, and M. Colombini, 2004 The Physiological

829 Properties of a Novel Family of VDAC-Like Proteins from Drosophila melanogaster.
830 Biophys. J. 86: 152–162. https://doi.org/10.1016/S0006-3495(04)74093-X
831 Kucherenko M. M., A. K. Marrone, V. M. Rishko, H. de F. Magliarelli, and H. R. Shcherbata,
832 2011 Stress and muscular dystrophy: A genetic screen for Dystroglycan and Dystrophin
833 interactors in Drosophila identifies cellular stress response components. Dev. Biol. 352:
834 228–242. https://doi.org/10.1016/J.YDBIO.2011.01.013
835 Kurusu M., A. Cording, M. Taniguchi, K. Menon, E. Suzuki, *et al.*, 2008 A Screen of Cell-Surface
836 Molecules Identifies Leucine-Rich Repeat Proteins as Key Mediators of Synaptic Target
837 Selection. Neuron 59: 972–985. https://doi.org/10.1016/J.NEURON.2008.07.037
838 Landis G. N., D. Bhole, and J. Tower, 2003 A search for doxycycline-dependent mutations that
839 increase Drosophila melanogaster life span identifies the VhaSFD, Sugar baby, filamin, fwd
840 and Cctlgenes. Genome Biol. 2003 42 4: 1–14. https://doi.org/10.1186/GB-2003-4-2-R8
841 Lavoy S., V. G. Chittoor-Vinod, C. Y. Chow, and I. Martin, 2018 Genetic Modifiers of
842 Neurodegeneration in a Drosophila Model of Parkinson's Disease. Genetics 209: 1345–
843 1356. https://doi.org/10.1534/genetics.118.301119
844 Lee G., and J. H. Park, 2004 Hemolymph Sugar Homeostasis and Starvation-Induced
845 Hyperactivity Affected by Genetic Manipulations of the Adipokinetic Hormone-Encoding
846 Gene in Drosophila melanogaster. Genetics 167: 311–323.
847 https://doi.org/10.1534/GENETICS.167.1.311
848 Li X., S. Zhang, G. Blander, J. Tse, M. Krieger, *et al.*, 2007 SIRT1 deacetylates and positively
849 regulates the nuclear receptor LXR. Mol. Cell 28: 91–106.
850 https://doi.org/10.1016/J.MOLCEL.2007.07.032
851 Lizák B., A. Szarka, Y. Kim, K. Choi, C. E. Németh, *et al.*, 2019 Glucose Transport and
852 Transporters in the Endomembranes. Int. J. Mol. Sci. 20.
853 https://doi.org/10.3390/IJMS20235898
854 Loubéry S., C. Seum, A. Moraleda, A. Daeden, M. Fürthauer, *et al.*, 2014 Uninflatable and

855 Notch Control the Targeting of Sara Endosomes during Asymmetric Division. Curr. Biol. 24:
856 2142–2148. https://doi.org/10.1016/J.CUB.2014.07.054
857 Lu J., S. J. Marygold, W. H. Gharib, and B. Suter, 2016 The aminoacyl-tRNA synthetases of
858 Drosophila melanogaster. https://doi.org/10.1080/19336934.2015.1101196 9: 53–61.
859 https://doi.org/10.1080/19336934.2015.1101196
860 Luo C.-W., E. M. Dewey, S. Sudo, J. Ewer, S. Y. Hsu, *et al.*, 2005 Bursicon, the insect cuticle-
861 hardening hormone, is a heterodimeric cystine knot protein that activates G protein-
862 coupled receptor LGR2. Proc. Natl. Acad. Sci. 102: 2820–2825.
863 https://doi.org/10.1073/PNAS.0409916102
864 Mackay T. F. C., S. Richards, E. A. Stone, A. Barbadilla, J. F. Ayroles, *et al.*, 2012 The
865 Drosophila melanogaster Genetic Reference Panel. Nature 482: 173–178.
866 https://doi.org/10.1038/nature10811
867 May C. E., A. Vaziri, Y. Q. Lin, O. Grushko, M. Khabiri, *et al.*, 2019 High Dietary Sugar
868 Reshapes Sweet Taste to Promote Feeding Behavior in Drosophila melanogaster. Cell
869 Rep. 27: 1675-1685.e7. https://doi.org/10.1016/J.CELREP.2019.04.027
870 McMullen E., A. Weiler, H. M. Becker, and S. Schirmeier, 2021 Plasticity of Carbohydrate
871 Transport at the Blood-Brain Barrier. Front. Behav. Neurosci. 0: 271.
872 https://doi.org/10.3389/FNBEH.2020.612430
873 Millington J. W., and E. J. Rideout, 2018 Sex differences in Drosophila development and
874 physiology. Curr. Opin. Physiol. 6: 46–56. https://doi.org/10.1016/J.COPHYS.2018.04.002
875 Montojo J., K. Zuberi, H. Rodriguez, F. Kazi, G. Wright, *et al.*, 2010 GeneMANIA Cytoscape
876 plugin: fast gene function predictions on the desktop. Bioinformatics 26: 2927–8.
877 https://doi.org/10.1093/bioinformatics/btq562
878 Nelson C. S., J. N. Beck, K. A. Wilson, E. R. Pilcher, P. Kapahi, *et al.*, 2016 Cross-phenotype
879 association tests uncover genes mediating nutrient response in Drosophila. BMC
880 Genomics 17. https://doi.org/10.1186/s12864-016-3137-9

881 Nogueiras R., K. M. Habegger, N. Chaudhary, B. Finan, A. S. Banks, *et al.*, 2012 Sirtuin 1 and
882 sirtuin 3: Physiological modulators of metabolism. Physiol. Rev. 92: 1479–1514.
883 https://doi.org/10.1152/physrev.00022.2011
884 Oas S. T., A. L. Bryantsev, and R. M. Cripps, 2014 Arrest is a regulator of fiber-specific
885 alternative splicing in the indirect flight muscles of Drosophila. J. Cell Biol. 206: 895–908.
886 https://doi.org/10.1083/JCB.201405058
887 Owusu-Ansah E., and N. Perrimon, 2014 Modeling metabolic homeostasis and nutrient sensing
888 in Drosophila: implications for aging and metabolic diseases. Dis. Model. Mech. 7: 343–
889 350. https://doi.org/10.1242/DMM.012989
890 Paik D., Y. G. Jang, Y. E. Lee, Y. N. Lee, R. Yamamoto, *et al.*, 2012 Misexpression screen
891 delineates novel genes controlling Drosophila lifespan. Mech. Ageing Dev. 133: 234–245.
892 https://doi.org/10.1016/J.MAD.2012.02.001
893 Palu R. A. S., and C. S. Thummel, 2016 Sir2 Acts through Hepatocyte Nuclear Factor 4 to
894 maintain insulin Signaling and Metabolic Homeostasis in Drosophila. PLoS Genet. 12: 1–
895 18. https://doi.org/10.1371/journal.pgen.1005978
896 Palu R. A. S., and C. Y. Chow, 2018 Baldspot/ELOVL6 is a conserved modifier of disease and
897 the ER stress response. PLoS Genet. 14. https://doi.org/10.1101/261206
898 Palu R. A. S., E. Ong, K. Stevens, S. Chung, K. G. Owings, *et al.*, 2019 Natural Genetic
899 Variation Screen in Drosophila Identifies Wnt Signaling, Mitochondrial Metabolism, and
900 Redox Homeostasis Genes as Modifiers of Apoptosis. G3 Genes|Genomes|Genetics 9:
901 g3.400722.2019. https://doi.org/10.1534/g3.119.400722
902 Palu R. A. S., H. M. Dalton, and C. Y. Chow, 2020 Decoupling of Apoptosis from Activation of
903 the ER Stress Response by the Drosophila Metallopeptidase superdeath. Genetics 214:
904 913–925. https://doi.org/10.1534/GENETICS.119.303004
905 Park J. W., K. Parisky, A. M. Celotto, R. A. Reenan, and B. R. Graveley, 2004 Identification of
906 alternative splicing regulators by RNA interference in Drosophila. Proc. Natl. Acad. Sci.

907 101: 15974–15979. https://doi.org/10.1073/PNAS.0407004101
908 Picard F., M. Kurtev, N. Chung, A. Topark-Ngarm, T. Senawong, *et al.*, 2004 Sirt1 promotes fat
909 mobilization in white adipocytes by repressing PPAR-gamma. Nature 429: 771–776.
910 https://doi.org/10.1038/NATURE02583
911 Prakash S., J. C. Caldwell, D. F. Eberl, and T. R. Clandinin, 2005 Drosophila N-cadherin
912 mediates an attractive interaction between photoreceptor axons and their targets. Nat.
913 Neurosci. 2005 84 8: 443–450. https://doi.org/10.1038/nn1415
914 Prisco G. Di, V. Cavaliere, D. Annoscia, P. Varricchio, E. Caprio, *et al.*, 2013 Neonicotinoid
915 clothianidin adversely affects insect immunity and promotes replication of a viral pathogen
916 in honey bees. Proc. Natl. Acad. Sci. 110: 18466–18471.
917 https://doi.org/10.1073/PNAS.1314923110
918 Queitsch C., K. D. Carlson, and S. Girirajan, 2012 Lessons from model organisms: phenotypic
919 robustness and missing heritability in complex disease. PLoS Genet 8: e1003041.
920 https://doi.org/10.1371/journal.pgen.1003041
921 Rabelink T. J., B. M. van den Berg, M. Garsen, G. Wang, M. Elkin, *et al.*, 2017 Heparanase:
922 roles in cell survival, extracellular matrix remodelling and the development of kidney
923 disease. Nat. Rev. Nephrol. 2017 134 13: 201–212. https://doi.org/10.1038/nrneph.2017.6
924 Rao Y., P. Pang, W. Ruan, D. Gunning, and S. L. Zipursky, 2000 brakeless is required for
925 photoreceptor growth-cone targeting in Drosophila. Proc. Natl. Acad. Sci. 97: 5966–5971.
926 https://doi.org/10.1073/PNAS.110135297
927 Reis T., M. R. Van Gilst, and I. K. Hariharan, 2010 A Buoyancy-Based Screen of Drosophila
928 Larvae for Fat-Storage Mutants Reveals a Role for Sir2 in Coupling Fat Storage to Nutrient
929 Availability, (E. Rulifson, Ed.). PLoS Genet. 6: e1001206.
930 https://doi.org/10.1371/journal.pgen.1001206
931 Rine J., and I. Herskowitz, 1987 Four Genes Responsible for a Position Effect on Expression
932 from HML and HMR in Saccharomyces cerevisiae. Genetics 116: 9.

933 Rodgers J. T., and P. Puigserver, 2007 Fasting-dependent glucose and lipid metabolic
934 response through hepatic sirtuin 1. Proc. Natl. Acad. Sci. U. S. A. 104: 12861–12866.
935 https://doi.org/10.1073/pnas.0702509104
936 Shannon P., A. Markiel, O. Ozier, N. S. Baliga, J. T. Wang, *et al.*, 2003 Cytoscape: a software
937 environment for integrated models of biomolecular interaction networks. Genome Res. 13:
938 2498–504. https://doi.org/10.1101/gr.1239303
939 Shlevkov E., and G. Morata, 2012 A dp53/JNK-dependant feedback amplification loop is
940 essential for the apoptotic response to stress in Drosophila. Cell Death Differ. 19: 451–460.
941 https://doi.org/10.1038/cdd.2011.113
942 Shore D., M. Squire, and K. A. Nasmyth, 1984 Characterization of two genes required for the
943 position-effect control of yeast mating-type genes. EMBO J. 3: 2817.
944 Sieber M. H., and C. S. Thummel, 2009 The DHR96 Nuclear Receptor Controls Triacylglycerol
945 Homeostasis in Drosophila. Cell Metab. 10: 481–490.
946 https://doi.org/10.1016/J.CMET.2009.10.010
947 Sivachenko A., H. B. Gordon, S. S. Kimball, E. J. Gavin, J. L. Bonkowsky, *et al.*, 2016
948 Neurodegeneration in a Drosophila model of adrenoleukodystrophy: the roles of the
949 Bubblegum and Double bubble acyl-CoA synthetases. Dis. Model. Mech. 9: 377–387.
950 https://doi.org/10.1242/DMM.022244
951 Somogyi K., B. Sipos, Z. Pénzes, and I. Andó, 2010 A conserved gene cluster as a putative
952 functional unit in insect innate immunity. FEBS Lett. 584: 4375–4378.
953 https://doi.org/10.1016/J.FEBSLET.2010.10.014
954 Spletter M. L., C. Barz, A. Yeroslaviz, C. Schönbauer, I. R. S. Ferreira, *et al.*, 2015 The RNA-
955 binding protein Arrest (Bruno) regulates alternative splicing to enable myofibril maturation
956 in Drosophila flight muscle. EMBO Rep. 16: 178–191.
957 https://doi.org/10.15252/EMBR.201439791
958 Subramanian A., P. Tamayo, V. K. Mootha, S. Mukherjee, B. L. Ebert, *et al.*, 2005 Gene set

959 enrichment analysis: a knowledge-based approach for interpreting genome-wide
960 expression profiles. Proc. Natl. Acad. Sci. U. S. A. 102: 15545–50.
961 https://doi.org/10.1073/pnas.0506580102
962 Talsness D. M., K. G. Owings, E. Coelho, G. Mercenne, J. M. Pleinis, *et al.*, 2020 A drosophila
963 screen identifies nkcc1 as a modifier of ngly1 deficiency. Elife 9: 1–22.
964 https://doi.org/10.7554/ELIFE.57831
965 Tennessen J. M., W. E. Barry, J. Cox, and C. S. Thummel, 2014 Methods for studying
966 metabolism in Drosophila. Methods 68: 105–115.
967 https://doi.org/10.1016/j.ymeth.2014.02.034
968 Udler M. S., M. I. McCarthy, J. C. Florez, and A. Mahajan, 2019 Genetic Risk Scores for
969 Diabetes Diagnosis and Precision Medicine. Endocr. Rev. 40: 1500–1520.
970 https://doi.org/10.1210/er.2019-00088
971 Wu H., and C. M. Ballantyne, 2020 Metabolic Inflammation and Insulin Resistance in Obesity.
972 Circ. Res. 126: 1549. https://doi.org/10.1161/CIRCRESAHA.119.315896
973 Yang J., X. Kong, M. Martins-Santos, G. Aleman, E. Chaco, *et al.*, 2009 Activation of SIRT1 by
974 resveratrol represses transcription of the gene for the cytosolic form of
975 phosphoenolpyruvate carboxykinase (GTP) by deacetylating hepatic nuclear factor 4alpha.
976 J. Biol. Chem. 284: 27042–27053. https://doi.org/10.1074/JBC.M109.047340
977 Zhao Y., J. Wei, X. Hou, H. Liu, F. Guo, *et al.*, 2017 SIRT1 rs10823108 and FOXO1
978 rs17446614 responsible for genetic susceptibility to diabetic nephropathy. Sci. Reports
979 2017 71 7: 1–9. https://doi.org/10.1038/s41598-017-10612-7
980 Zhou X., and M. Stephens, 2012 Genome-wide efficient mixed-model analysis for association
981 studies. Nat. Genet. 44: 821–4. https://doi.org/10.1038/ng.2310
982 Zhou X., C. J. Guo, H. H. Hu, J. Zhong, Q. Sun, *et al.*, 2019 Drosophila CTP synthase can form
983 distinct substrate- and product-bound filaments. J. Genet. Genomics 46: 537–545.
984 https://doi.org/10.1016/J.JGG.2019.11.006

985 Zillikens M. C., J. B. J. van Meurs, F. Rivadeneira, N. Amin, A. Hofman, *et al.*, 2009 SIRT1
986 Genetic Variation Is Related to BMI and Risk of Obesity. Diabetes 58: 2828–2834.
987 https://doi.org/10.2337/DB09-0536
988

989 **FIGURE LEGENDS**

990 **Figure 1. Glucose levels vary under a variety of environmental conditions.**
991 Glucose levels were measured in three samples for each of 30-36 strains under one of the
992 indicated conditions: one week of adult age and fed ad libitum (N = 30 strains, P = 1.87E-05)
993 (**A**), one week of adult age and fasted for 12-13 hours (N = 30 strains, P = 0.0194) (**B**), two
994 weeks of adult age and fed ad libitum (N = 30 strains, P = 0.0103) (**C**), and two weeks of adult
995 age and fasted for 12-13 hours (N = 36 strains, P = 1.95E-05) (**D**). Mean glucose concentrations
996 are indicated, with error bars indicating standard deviation. DGRP strain or RAL numbers are
997 indicated along the X-axis. P-values were calculated using one-way ANOVA incorporating all
998 individual measurements comparing DGRP strain with glucose concentration. Adult flies were
999 collected within 2-3 days after eclosion from the pupal case and aged to the indicated time
1000 points. * P < 0.05, **** P < 5E-05.
1001

1002 **Figure 2. Glucose levels are significantly affected by genetic background.**
1003 Glucose levels were measured in three samples for each of 185 strains at two weeks of age
1004 after a 12 hour fast. Adult flies were collected within 2-3 days after eclosion from the pupal case
1005 and aged an additional 9-11 days prior to fasting (11-14 days post-eclosion). Flies were
1006 collected after the overnight fast at 12-15 days post-eclosion. Mean glucose concentrations are
1007 indicated, with error bars indicating standard deviation. P-values were calculated using one-way
1008 ANOVA incorporating all individual measurements comparing DGRP strain with glucose
1009 concentration (P < 2E-16).
1010

1011 **Figure 3. Immune responses, neuronal function, and basic metabolic processes are**
1012 **overrepresented in GWA candidate modifiers of hyperglycemia.**
1013 (**A**) *R4>Sirt1i* modifier network, as plotted by the GeneMANIA plugin in Cytoscape (Shannon *et*
1014 *al.* 2003; Montojo *et al.* 2010). Significant candidate modifiers are indicated in red, with physical
1015 interactions indicated by connecting red lines. Thicker lines indicate stronger evidence for the
1016 interaction. Encircled genes share common pathways or functions. Interacting genes outside of
1017 the candidate modifier list are indicated in gray. (**B**) Top 20 significant ontological categories as
1018 identified by GSEA. Categories are arranged from most significant on top to least significant
1019 along the y-axis. P-values are indicated by red-to-blue gradient, with red the lowest p-values
1020 and blue the highest P-values. Enrichment score (ES) for each category is plotted along the x-
1021 axis. Gene number identified in each category is indicated by dot size.
1022
1023 **Figure 4. Loss of candidate gene expression suppresses hyperglycemia in the R4>Sirt1i**
1024 **model**
1025 RNAi against candidate modifiers was expressed under the control of *R4-GAL4* in the *R4>Sirt1i*
1026 model. Glucose level for each sample was normalized to the levels in a genetically matched
1027 control line crossed into the *R4-Sirt1* line. Average *R4>Sirt1i* control glucose levels after
1028 normalization are indicated by a dotted line at 1.0, with standard deviation highlighted by the gray
1029 box. Whole fly glucose concentration was quantified for N = 4-5 samples per strain, each
1030 consisting of 5 flies and individually plotted along the y-axis. Knockdown of *CG4168, CG5888*, or
1031 *uif* significantly reduces glucose concentrations in the *R4>Sirt1i* model of hyperglycemia
1032 compared to controls (blue). Loss of *CTPSyn* does not significantly alter glucose levels, but a
1033 trending decrease in glucose levels were observed in several independent RNAi strains (light
1034 blue, data not shown). Loss of *smt3*, *ilp5*, *snRNP-U1-70k*, *CG10265*, *CG15803*, *Roe*, *CG34353*,
1035 *CadN2*, *CG43897*, *CG3407*, *dsxc73A*, or *bgm* do not produce a significant effect (dark gray). P-

1036 values were calculated using one-way ANOVA followed by Dunnett's multiple testing correction.

1037 * $P < 0.05$, *** $P < 0.001$.

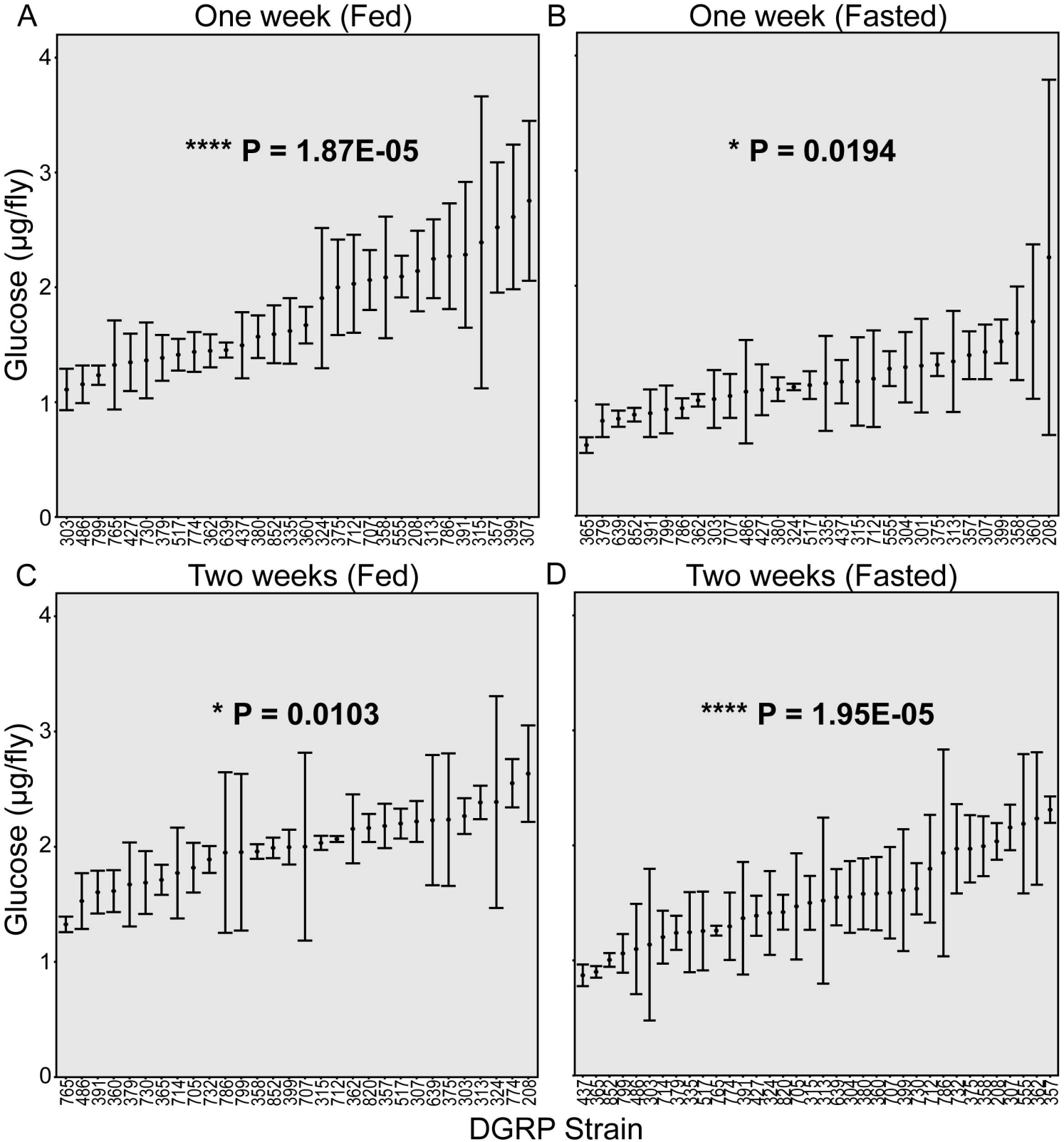
A
One week (Fed)
**** P = 1.87E-05
B
One week (Fasted)
* P = 0.0194
C
Two weeks (Fed)
* P = 0.0103
D
Two weeks (Fasted)
**** P = 1.95E-05
Glucose (µg/fly)
0
1
2
3
4
303 486 799 765 427 730 379 517 774 362 639 437 380 852 335 360 324 375 712 707 358 555 208 313 786 391 315 357 399 307
365 379 639 852 391 799 786 362 303 707 486 427 380 324 517 335 437 315 712 555 304 301 375 313 357 307 399 358 360 208
765 486 391 360 379 730 365 714 705 732 786 799 358 852 399 707 315 712 362 820 357 517 307 639 375 303 313 324 774 208
437 365 852 799 486 303 714 379 375 335 517 765 774 391 427 324 820 705 315 313 639 304 380 360 707 399 730 712 786 792 775 358 208 307 555 362 357
DGRP Strain

Figure 1.

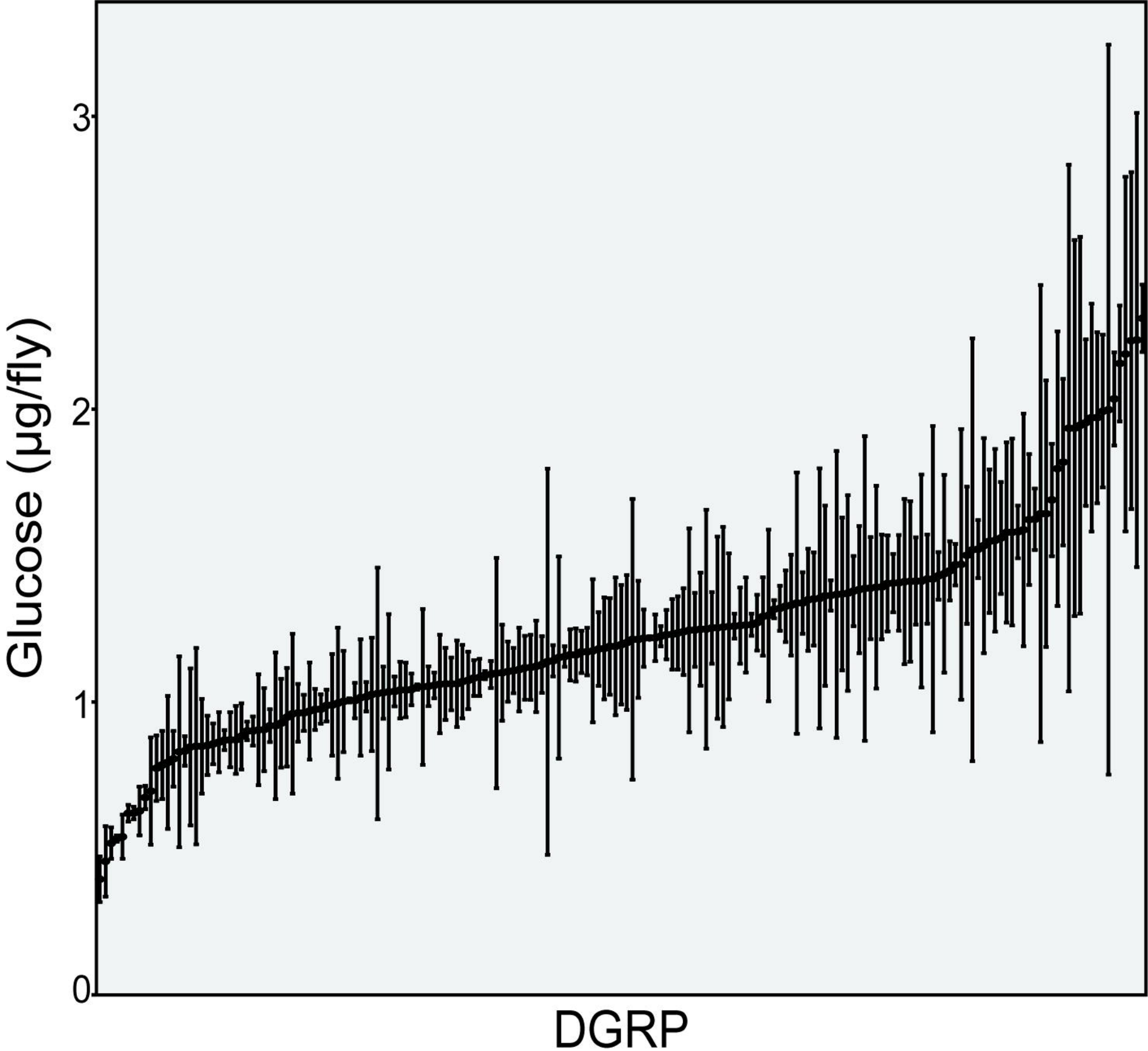

Figure 2

A

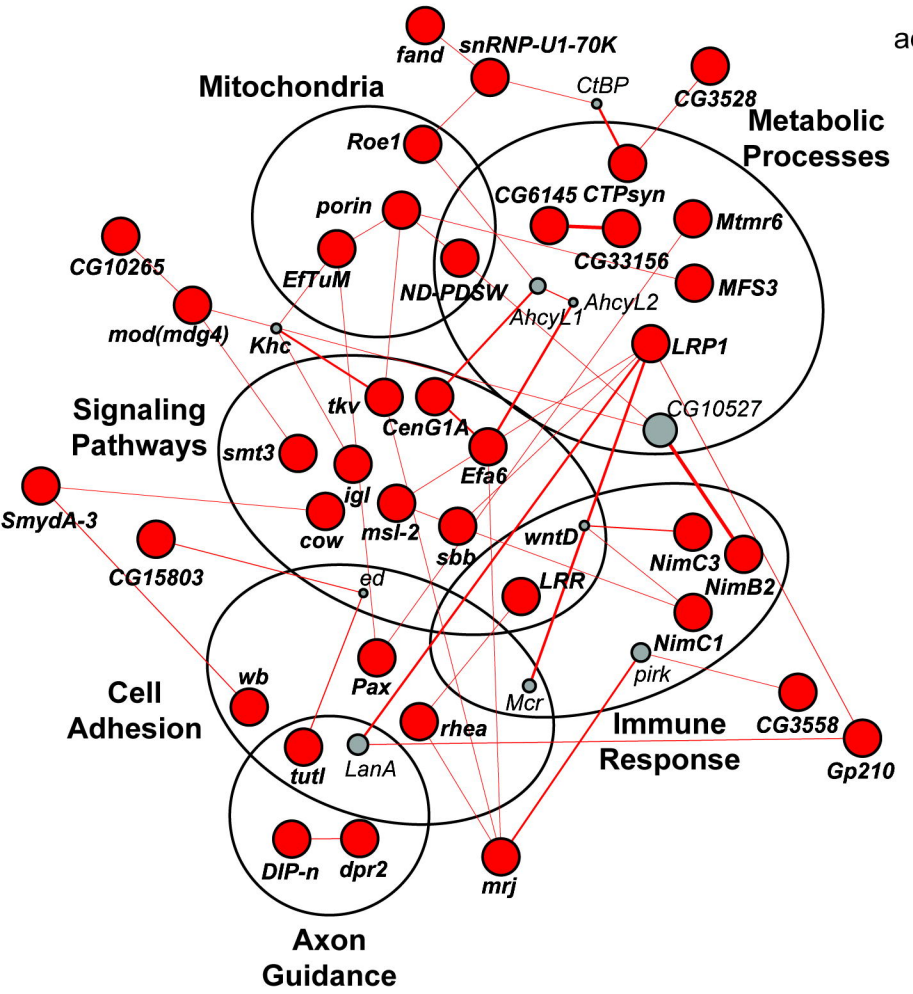
Mitochondria
Metabolic Processes
Signaling Pathways
Cell Adhesion
Immune Response
Axon Guidance
fand
snRNP-U1-70K
CtBP
CG3528
Roe1
CG6145
CTPsyn
porin
Mtmr6
CG33156
CG10265
EfTuM
ND-PDSW
MFS3
AhcyL1
AhcyL2
mod(mdg4)
Khc
LRP1
tkv
CenG1A
CG10527
smt3
Efa6
igl
SmydA-3
cow
msl-2
sbb
wntD
NimC3
CG15803
ed
LRR
NimB2
NimC1
pirk
wb
Pax
Mcr
rhea
CG3558
tutl
LanA
Gp210
DIP-n
dpr2
mrj

B

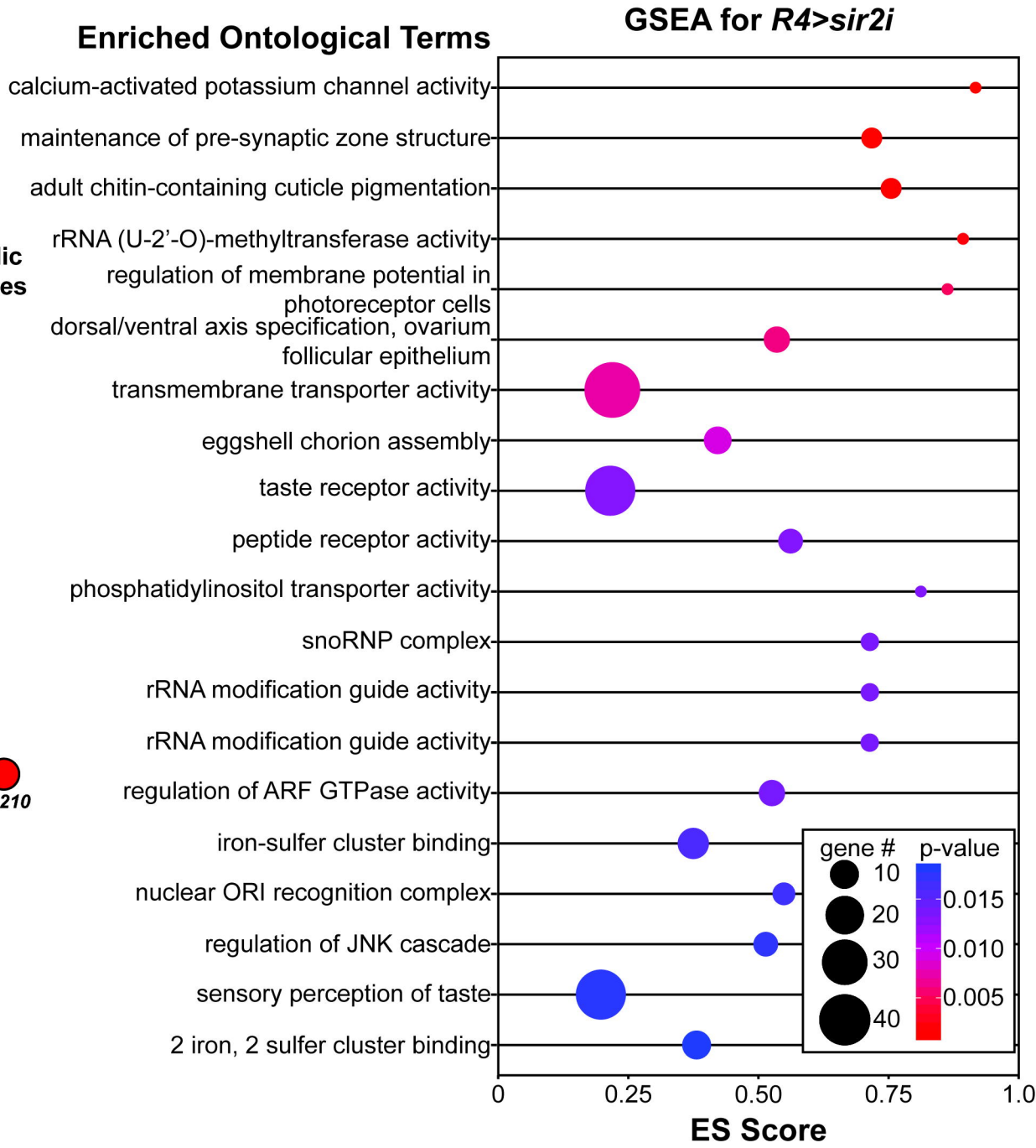
GSEA for R4>sir2i
Enriched Ontological Terms
calcium-activated potassium channel activity
maintenance of pre-synaptic zone structure
adult chitin-containing cuticle pigmentation
rRNA (U-2'-O)-methyltransferase activity
regulation of membrane potential in photoreceptor cells
dorsal/ventral axis specification, ovarium follicular epithelium
transmembrane transporter activity
eggshell chorion assembly
taste receptor activity
peptide receptor activity
phosphatidylinositol transporter activity
snoRNP complex
rRNA modification guide activity
rRNA modification guide activity
regulation of ARF GTPase activity
iron-sulfer cluster binding
nuclear ORI recognition complex
regulation of JNK cascade
sensory perception of taste
2 iron, 2 sulfer cluster binding
gene #
10
20
30
40
p-value
0.015
0.010
0.005
0
0.25
0.50
0.75
1.0
ES Score

Figure 3

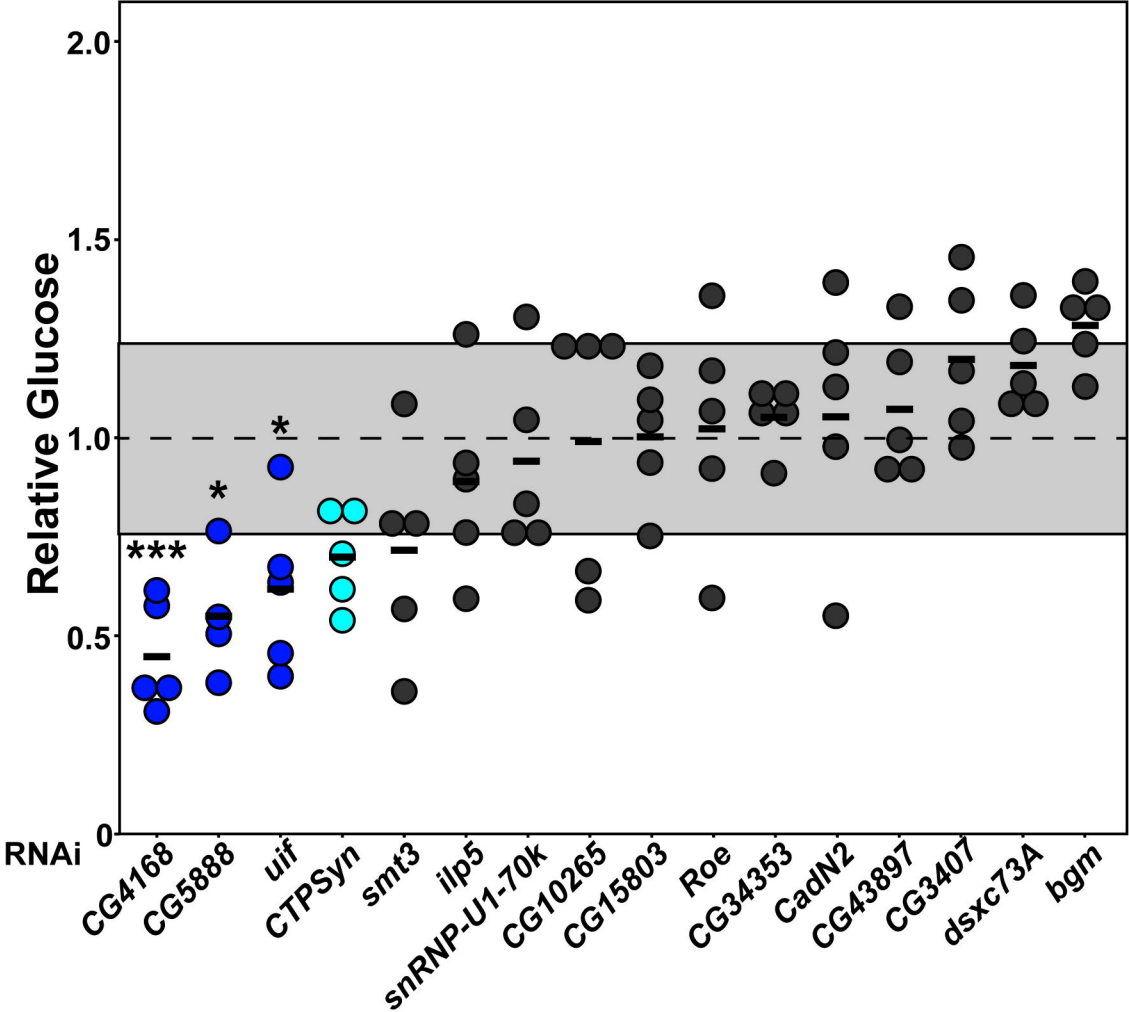
Relative Glucose
2.0
1.5
1.0
0.5
0
***
*
*
RNAi
CG4168
CG5888
uif
CTPSyn
smt3
ilp5
snRNP-U1-70k
CG10265
CG15803
Roe
CG34353
CadN2
CG43897
CG3407
dsxc73A
bgm

Figure 4